

PRELIMINARY CALCULATIONS OF EXPECTED DOSE FROM EXTRUSIVE VOLCANIC EVENTS AT YUCCA MOUNTAIN

Mark S. Jarzempa and Patrick A. LaPlante

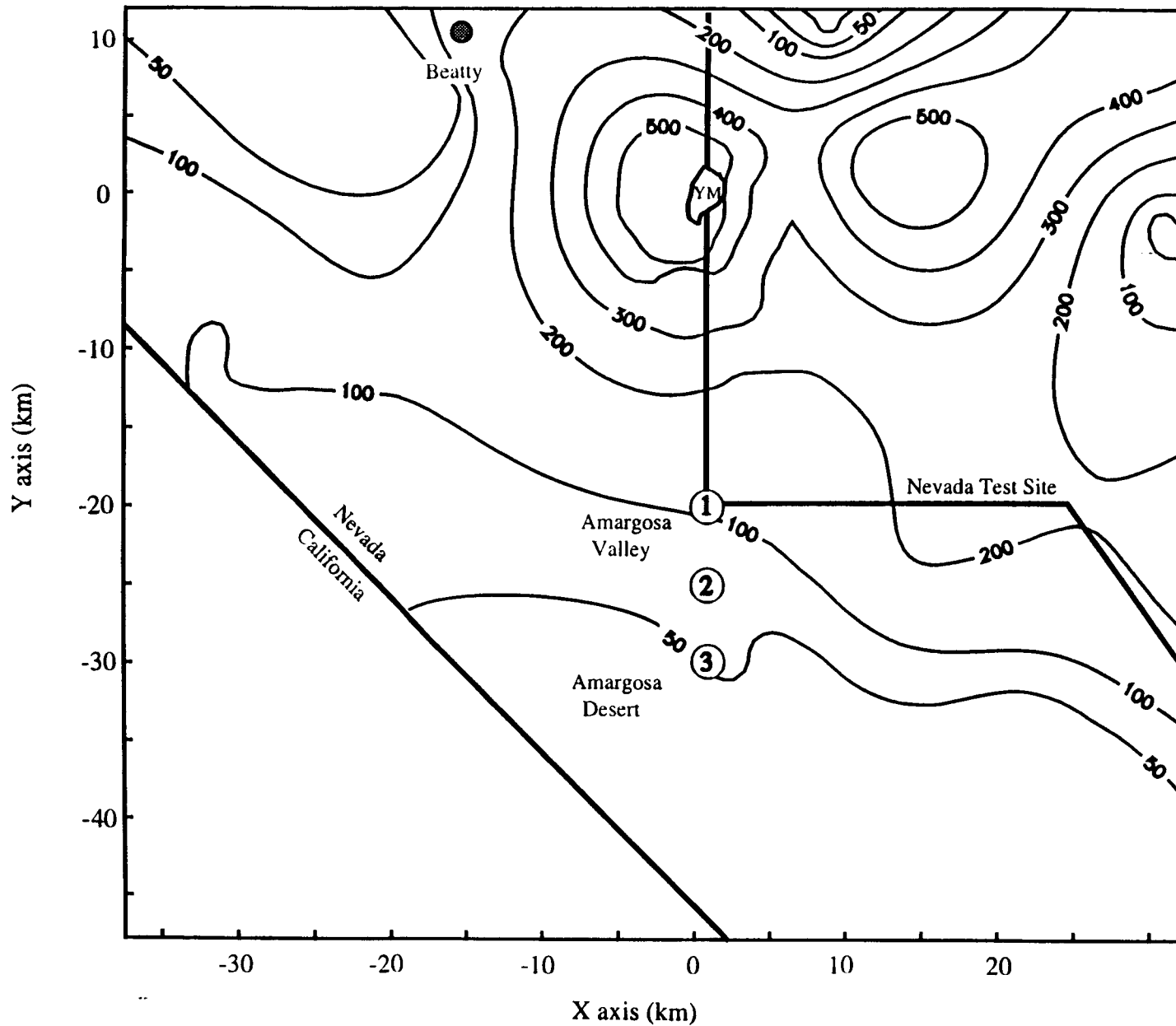
1 INTRODUCTION

The purpose of this report is to demonstrate a calculational technique and to provide a preliminary estimate of radiation doses for the scenario of extrusive volcanism at the Yucca Mountain (YM) site. Calculations are based in part on a probabilistic volcanic ash (tephra) distribution model developed by Suzuki (1983) and extended by Jarzempa (1996). In addition, a new model for distributing spent fuel within the ash particles has been developed to more realistically model (than previous methods) radionuclide distributions on the earth's surface after a volcanic event. Dose modeling of radiation exposures from the contaminated ash blanket has also been performed. The dose pathways considered in these analyses were: ingestion (from contaminated animal products and crops), inhalation from resuspension and external radiation. Dose Conversion Factors (DCFs) as a function of these important pathways, and as a total of all the pathways, were derived for contaminated soil in a manner similar to that described in LaPlante et al., (1995) for an Amargosa Desert farmer/rancher residing at the point of interest on the earth's surface (the dose point) immediately after the volcanic event occurs. The analyses herein were performed for two different time periods of interest: 10,000 yr and 1,000,000 yr.

2 DESCRIPTION OF MODELING APPROACH

2.1 EXPOSURE SCENARIO

The exposure scenario for these dose estimates is based on the assumption that the critical group is composed of an Amargosa Desert farmer/rancher residing on a plot of land at a specified point in the region (the dose point) immediately after a volcanic eruption occurs. The critical group is defined as a relatively small group of individuals (or individual) whose membership includes the maximally exposed individual, using cautious but reasonable assumptions, and other individuals whose projected dose is within an order of magnitude of the maximally exposed individual [(ICRP 1991; 1985; 1977)]. For the purposes of these analyses, the critical group is the maximally exposed individual as defined by the lifestyle characteristics in LaPlante et al., (1995). For these preliminary analyses, no other possible critical groups were considered. The Amargosa Desert farmer/rancher is selected as the critical group because of current lifestyle practices in the YM region. Figure 1 shows the dose points chosen for this report and the depth to the water table. The depth to the water table together with land slope were key parameters in deciding where this group would most likely exist. A great depth to the water table would make this scenario economically infeasible. Similarly, a high land slope would seem to limit the desirability of a sight for arid-region farming. Due to large uncertainties in predictions of parameter values over the long term, a static biosphere assumption was used that relies on current site characteristics, of the region south of YM for dose estimates (i.e., today's biosphere). Details of the farmer/ranchers lifestyle activities were based upon reasonable assumptions that would result in a



2

Figure 1. The dose points considered in these analyses; water table contours in meters below ground surface

3/1/8

reasonably maximal exposure. The resident farmer/rancher was assumed to raise (locally) half of his consumed beef, milk, fruit, grain, and vegetables and was assumed to obtain all pork, poultry, and fish products from other, uncontaminated sources. The assumption that the farmer/rancher consumes half of his beef, milk, fruit, grains, and vegetables is similar to assumptions made for low-level waste repository performance assessments where it is assumed that 50 percent of a person's diet is from contaminated, locally grown food [Yu et al., (1993)]. These assumptions are based on the best available site specific information about the lifestyle activities of this group [LaPlante et al., (1995), Wescott et al., (1995)]. A detailed description of the lifestyle characteristics of the exposure scenario and parameter selections is provided in LaPlante et al. (1995), however, the present analysis used soil concentration from volcanic ash deposition as the source of contamination rather than groundwater. In this region, no farms exist that sell food crops for export, but some raise livestock using both pasture land and feed crops irrigated with local groundwater.¹ The primary livestock in the county encompassing the potential exposure area are beef cattle, while hogs, chickens, and milk cows are raised in lesser numbers [U.S. Department of Commerce (1989)]. Feed crops are predominantly hay (e.g., alfalfa) and limited amounts of grain. At present, alfalfa farms in particular are located in the Amargosa Desert region [Nevada Division of Water Resources (1995)].

Parameter distributions were determined from the literature or estimated from reported ranges. Agricultural information was collected for southwestern Nevada [U.S. Department of Commerce (1989); Nevada Agricultural Statistics Service (1988)]. Soil characteristics were assumed to be similar to those in the Amargosa Desert area and information on these characteristics was obtained from local and national offices of the Soil Conservation Service [LaPlante et al. (1995)]. Future analyses may include updating these soil characteristics with ones more representative of volcanic ash.

Nevada Test site studies provided information for modeling doses from resuspension [Anspaugh et al. (1975); Otis (1983); Breshears et al. (1989)] and crop interception of contaminated air [Anspaugh (1987)]. For the present analysis, a resuspension factor for soil was used, however, future analyses may be improved by using resuspension factors for volcanic ash. A range from 30 to 82 percent of animal feed for milk and beef was assumed to be from contaminated fresh forage [Breshears et al. (1992)]. Generic parameter values from prior NRC assessments [Kennedy and Strenge (1992)] were used when information was not available from local sources. Food transfer factors, while not from local sources, were from recent work [International Atomic Energy Agency (1994)] supplemented as necessary with additional data [Baes III et al. (1982); Hoffman et al. (1982)]. External dose conversion factors in the GENII-S code [Leigh et al., (1993)] were updated using recent Environmental Protection Agency (EPA) federal guidance [Eckerman and Ryman (1993)].

A diagram of this exposure scenario is presented in Figure 2. The progression of events in the exposure scenario shown in Figure 2 is as follows:

- (1) Magma enters the repository and becomes contaminated with spent fuel particles.
- (2) Ash forms into contaminated particulate matter. The level of contamination of the particles as a function of particle size of the volcanic ash is as given later in this report.
- (3) Eruption parameters are sampled according to the procedure given in Jarzempa (1996).

¹Personal Communication, Las Vegas Agricultural Extension Office, Nevada, January 27, 1995.

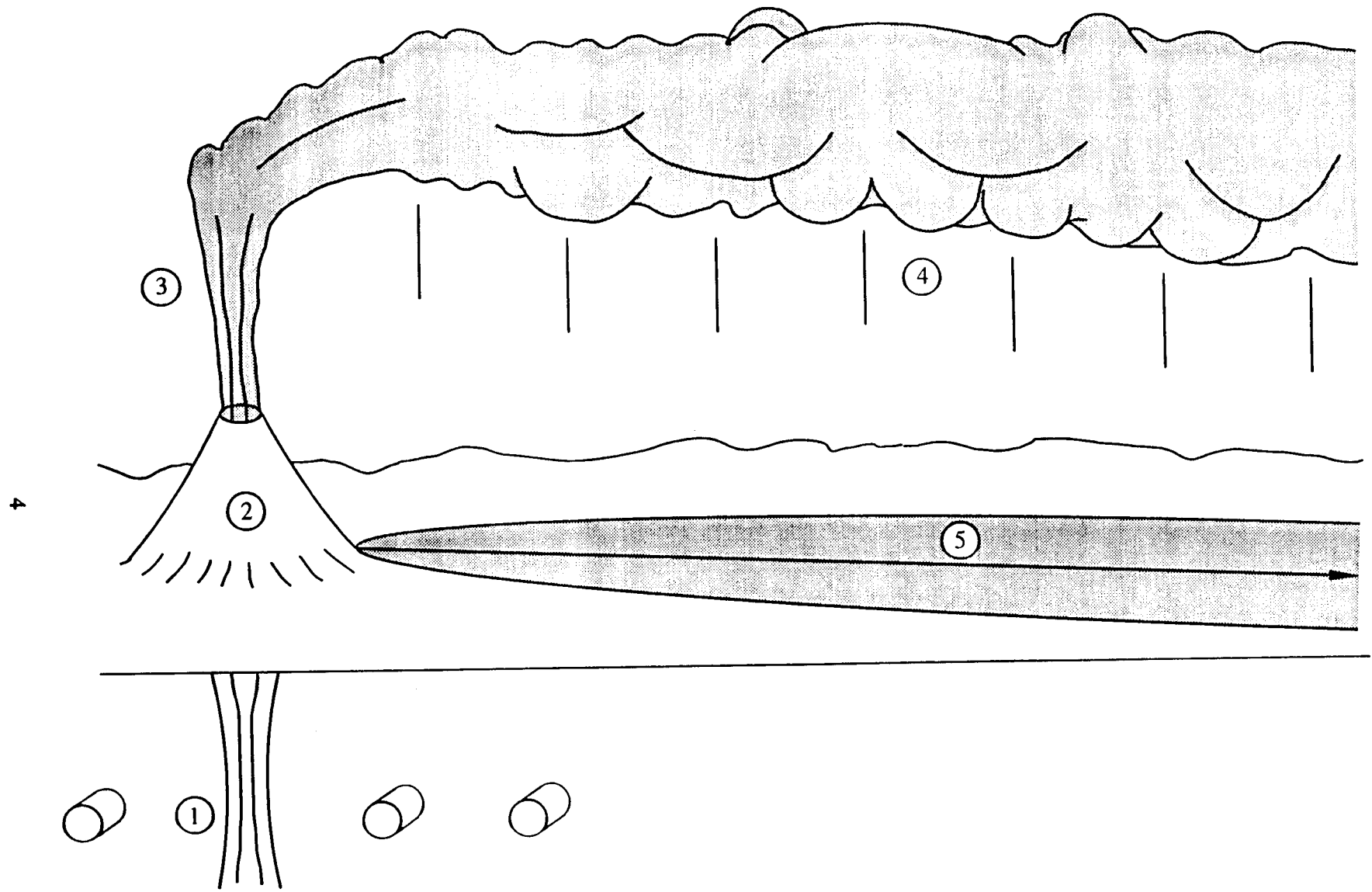


Figure 2. Diagram of the exposure scenario

5/4/1

- (4) Eruption column and contaminant plume form and produce volcanic ash fallout at distances and directions as determined by the methods in Suzuki (1983) and Jarzempa (1996).
- (5) Doses received by an Amargosa Desert farmer/rancher at the dose points were calculated. It is assumed that the farmer/rancher exists immediately after the particle plume laid down the contaminated blanket. The pathways accounted for in the calculated doses were inhalation (from resuspension), ingestion from both contaminated animal products and crops, and external dose from groundshine. Contamination of the water table from water percolating through the ash blanket and subsequent doses from the drinking water pathway have not been accounted for in these analyses.

2.2 PROBABILITY OF VOLCANIC DISRUPTION

In order to calculate the expected value of the peak dose to the critical group due to extrusive volcanism in the Time Period of Interest (TPI), the probability of volcanic disruption must be known. Connor and Hill (1995) modeled volcanism in the YM region as a spatially inhomogeneous and time homogeneous process to estimate the probability of a new cone forming in an 8 km² region, including the repository footprint plus a 500 m buffer zone, over the next 10,000 yr. They found that the probability ranges from about 1×10^{-4} to 5×10^{-4} . For the purposes of these analyses, a centroid value of 3×10^{-4} per 10,000 yr, leading to a recurrence rate (λ_{rr}) of 3×10^{-8} per yr was assumed.

Two TPIs were considered; 10,000 yr and 1,000,000 yr. Multiple events in the TPI were not explicitly considered, however, in determining the probability of new cone formation they were treated as a single event. If it is assumed that the above recurrence rate is constant in time (i.e., no waxing or waning) and that volcanism occurs as a homogeneous Poisson process, then the probability of no volcanic disruption in the TPI is given by:

$$\overline{p(TPI)} = \exp(-\lambda_{rr} \cdot TPI) \quad (2-1)$$

Conversely, the probability of at least one disruption during the TPI is given by:

$$p(TPI) = 1 - \exp(-\lambda_{RR} \cdot TPI) \quad (2-2)$$

Explicitly, the probabilities of at least one disruption in TPIs of 10,000 yr and 1,000,000 yr are:

$$p(10,000 \text{ yr}) = 3.0 \times 10^{-4} \quad (2-3)$$

$$p(1,000,000 \text{ yr}) = 3.0 \times 10^{-2} \quad (2-4)$$

2.3 VOLCANIC ASH DISTRIBUTION CALCULATIONS

Volcanic ash distributions after an event were calculated using the methods and data outlined in Jarzempa (1996). The point on the earth's surface at which volcanic ash thicknesses and subsequent radionuclide densities were calculated, (the dose point), was assumed to be at a specified location and is

7/41

treated as a parameter in these calculations. Possible dose points used in these calculations were 20, 25, and 30 km directly south of the repository. These points were chosen based on: knowledge of the present day population [LaPlante et al., (1995), Wescott et al., (1995)], depth to the water table, and land slopes considered to be favorable to farming/ranching under the present condition.

2.4 RADIONUCLIDE DISTRIBUTION WITHIN THE ASH BLANKET

In Jarzempa (1996), the radionuclides released in the volcanic event were assumed to be uniformly distributed within the volcanic ash mass released in the event. In these analyses, a different distribution was used, which is thought to be more realistic even though no experimental data is available to confirm this assertion.

Spent nuclear fuel is highly fractured from the buildup of fission fragment gasses in its ceramic matrix during irradiation in the reactor. Figure 3, abstracted from Clark et al., (1985), shows a cross section of an irradiated spent-fuel pellet. For these analyses, it was assumed that the log of the fuel particle diameter has a triangular probability distribution. The minimum and maximum fuel particle diameters were assumed to be 0.01 cm and 1.0 cm which correspond to log-diameters of -2 and 0 respectively. The median particle diameter was assumed to be 0.1 cm corresponding to a log-diameter of -1. Figure 4 shows the probability density function for the mass of fuel of the log-diameter $[m(\rho^f)]$ using these assumptions. The upper limit of $\rho^f = 0$ was assumed because spent-fuel pellets are about 1 cm in diameter before irradiation in the reactor. The median value of $\rho^f = -1$ was assumed from the visual evidence presented in Figure 3, as the median fractured particle diameter appears to be about 1 mm. The lower limit of $\rho^f = -2$ was assumed based on this same evidence since very few particles in Figure 3 appear to have diameters smaller than 0.1 mm. This distribution of the fuel particle size was used independent of the timing of the event. Future work on this topic may include use of a time dependent distribution of the fuel mass with particle size to account for changes in fuel structure with chemical composition and age.

It was conservatively assumed in these analyses that all canister cladding and containment have been breached and are ineffective at preventing exposure of the fuel to the magma or volcanic ash particulate matter as it is being formed. This assumption will be investigated further in future work on this topic. Since the magma is typically at temperatures of about 1,000 °C, which is above the melting point of zircalloy, the conservative assumption that the cladding was also ineffective at preventing spent-fuel incorporation was made. This assumption may also be updated as further information on waste package performance under these conditions becomes available.

This scheme for partitioning fuel into an erupting magma requires the introduction of a new function into the previous analyses of Jarzempa (1996) to determine the mass of fuel per unit mass of volcanic ash as a function of the log-diameter of the ash after the ash has been contaminated with spent fuel $[FF(\rho^a)]$. As in Jarzempa (1996), the volcanic ash mass is assumed to be distributed lognormally

$$f(\rho^a) = \frac{1}{\sqrt{2\pi}\sigma_d} \exp\left(-\frac{(\rho^a - \rho_{\text{mean}}^a)^2}{2\sigma_d^2}\right) \quad (2-5)$$

8/41

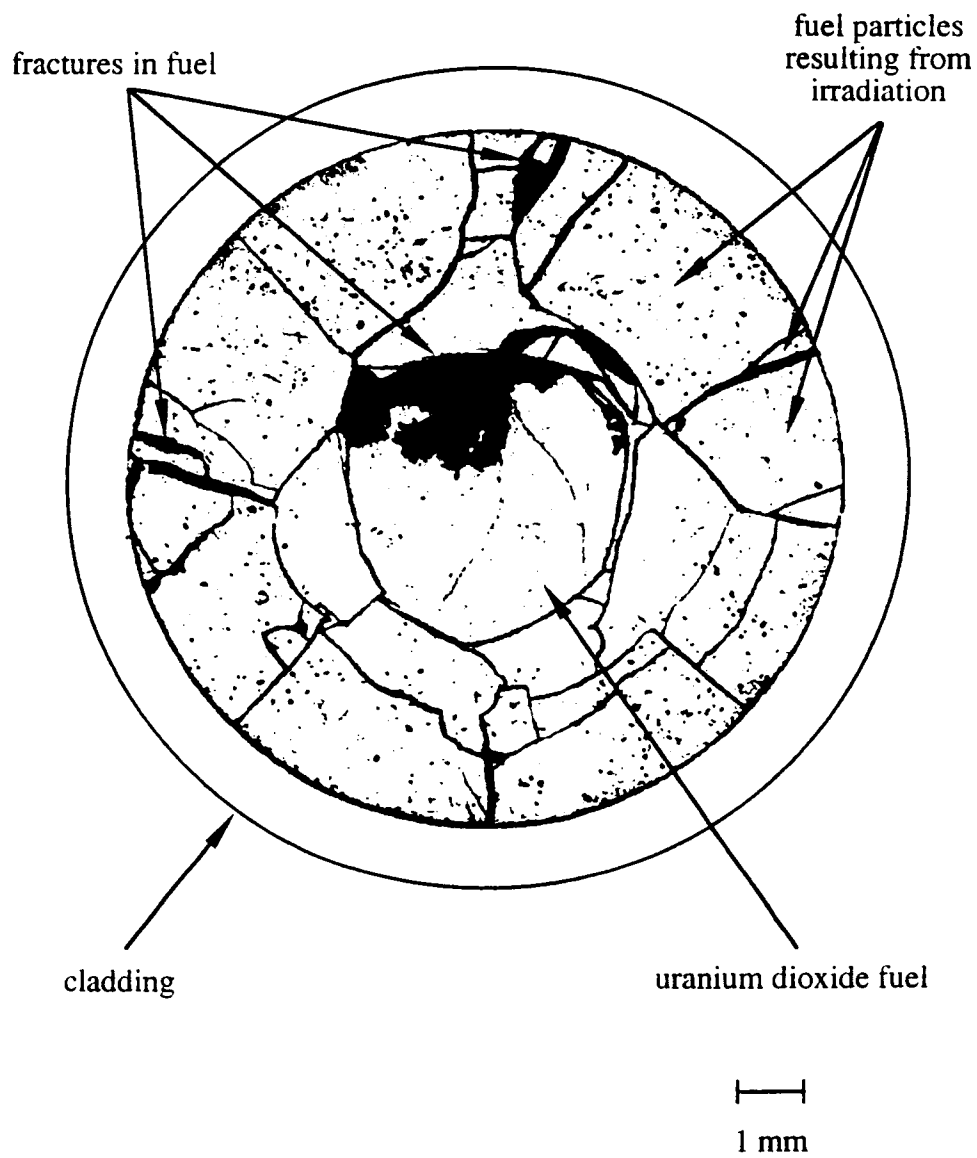


Figure 3. Cross-section of a fuel pellet after irradiation and fissioning in a reactor [abstracted from Clark, et al., (1985)]

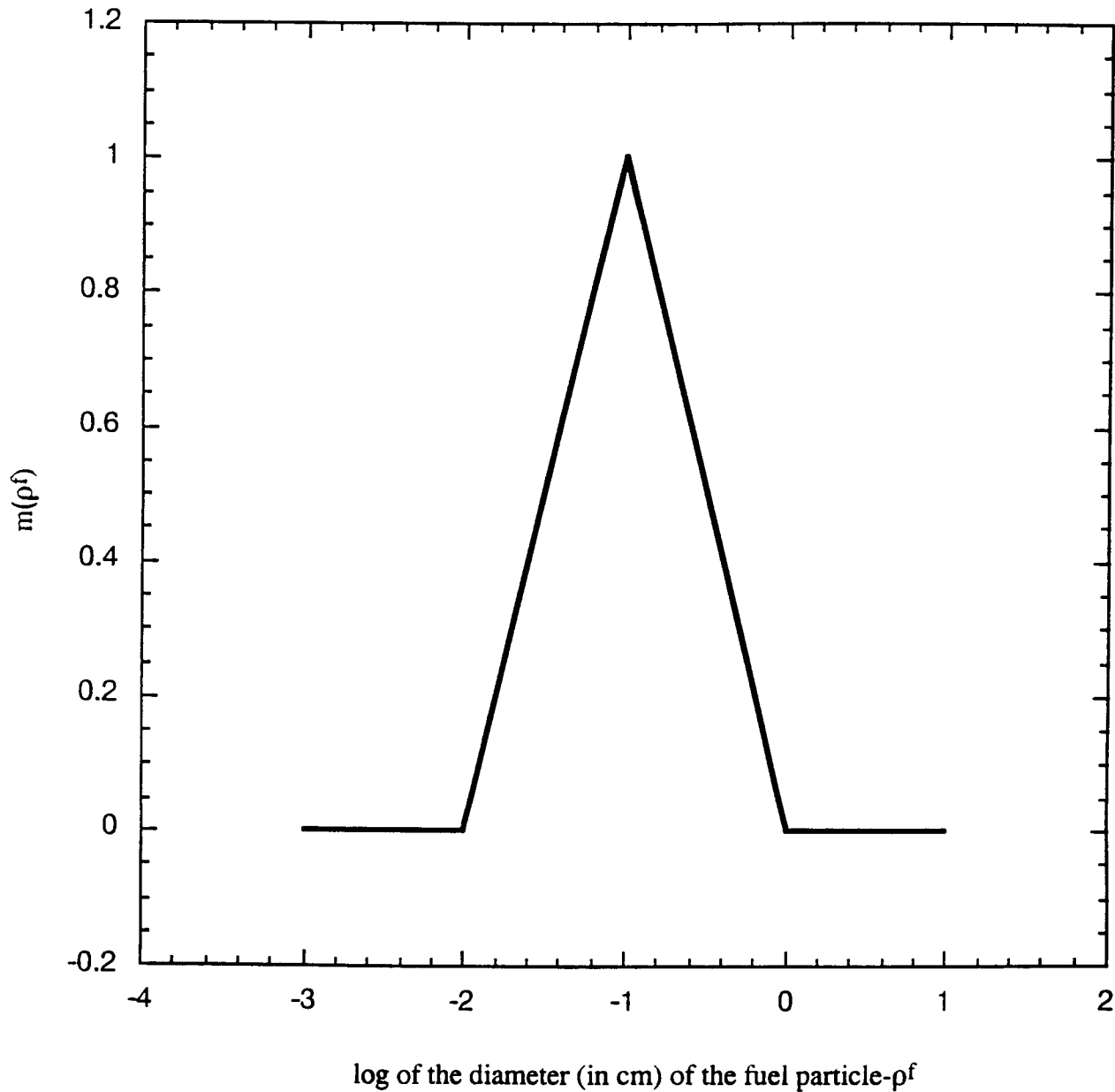


Figure 4. Assumed probability density of mass of fuel versus log-diameter of fuel particle

where:

- ρ^a = the log-diameter of ash particle size, with particle size in cm
- ρ_{mean}^a = the mean of the log-diameter of ash particle size, with particle size in cm
- σ_d = the standard deviation of the log particle size
- $f(\rho^a)$ = the normalized probability distribution of ash mass with ρ^a

The mass of fuel as a function of the log-diameter of the fuel $[m(\rho^f)]$ is defined as

$$\begin{aligned}
 m(\rho^f) &= k_1(\rho^f - \rho_{\text{min}}^f) && \rho_{\text{min}}^f < \rho^f \leq \rho_{\text{med}}^f \\
 m(\rho^f) &= k_2(\rho^f - \rho_{\text{med}}^f) + k_1(\rho_{\text{med}}^f - \rho_{\text{min}}^f) && \rho_{\text{med}}^f < \rho^f \leq \rho_{\text{max}}^f \\
 m(\rho^f) &= 0 && \text{otherwise}
 \end{aligned}
 \tag{2-6}$$

where:

$$k_1 = \frac{2}{(\rho_{\text{max}}^f - \rho_{\text{min}}^f)(\rho_{\text{med}}^f - \rho_{\text{min}}^f)}$$

$$k_2 = -\frac{2}{(\rho_{\text{max}}^f - \rho_{\text{min}}^f)(\rho_{\text{max}}^f - \rho_{\text{med}}^f)}$$

- ρ^f = the log-diameter of fuel particle size, with particle size in cm
- ρ_{min}^f = the minimum log-diameter of fuel particle size, with particle size in cm
- ρ_{max}^f = the maximum log-diameter of fuel particle size, with particle size in cm
- ρ_{med}^f = the median log-diameter of fuel particle size, with particle size in cm
- $m(\rho^f)$ = the normalized probability distribution of fuel mass with ρ^f

The motivation for limiting the amount of fuel mass available for incorporation into the volcanic ash particles of a given size is that for smaller volcanic ash particles an amount of fuel mass will be too large to be incorporated into these small particles. For example, a 1 cm fuel particle cannot be incorporated by a 0.5 cm volcanic ash particle. For the purposes of these analyses, the cutoff on the ratio of "incorporable" fuel diameter to volcanic ash diameter was assumed to be 0.1. This assumption means that the incorporable fuel mass must have a log-diameter (ρ^f) less than $\rho^a - \rho_c$ where ρ_c is equal to one. The parameter ρ_c can be revised as future information becomes available. A sensitivity analysis of ρ_c may also be conducted to determine the importance of this parameter. Another example, ρ_c equal to zero,

is equivalent to allowing all fuel mass of size less than or equal to the volcanic ash particle size to be available for incorporation.

The assumption that ρ_c is equal to one was made from the authors' observations of actual particles presumably transported by volcanic convective columns and subsequent plume fallout. The observed incorporated matter (wall or other rock fragments) in these particles appears to be about one order of magnitude or less in size than the particle size itself.

To determine $FF(\rho^a)$ the fuel fraction (ratio of fuel mass to ash mass) as a function of ρ^a , one must consider that all fuel particles of size smaller than $(\rho^a - \rho_c)$ have the ability to simultaneously be incorporated into volcanic ash particles of size ρ^a or larger. This situation is shown in Figure 5 by considering that all the fuel mass in area 1 of the lower curve is available to all the volcanic ash mass in area 1 of the upper curve. Similarly, all the fuel mass in area 2 of the lower curve is available to all the volcanic ash mass in area 2 of the upper curve. This partitioning scheme was done to reflect the fact that larger volcanic ash has the ability to incorporate a relatively larger amount of spent-fuel. The fuel fraction as a function of ρ^a was determined by summing all the incremental contributions of fuel mass to the volcanic ash mass from fuel sizes smaller than $(\rho^a - \rho_c)$. An expression for the fuel fraction is given as

$$FF(\rho^a) = \frac{U}{q} \cdot \int_{\rho - \rho_c}^{\rho^a} \frac{m(\rho - \rho_c)}{1 - F(\rho)} d\rho$$

(2-7)

where:

- q = the total mass of ash ejected in the event in g
- U = the total mass of fuel ejected in the event in g
- $F(\rho^a)$ = the cumulative distribution of $f(\rho^a)$

Equation (2-7) assumes the resulting contaminated particles follow the same size distribution as the original volcanic ash particles. This seems reasonable since for most events sampled in these analyses, the total mass of volcanic ash is on the order of 10^{13} to 10^{15} g and for these preliminary analyses, each event was assumed to disrupt one waste package, or 10^7 g of fuel. The assumption that one waste package was available for incorporation was used as a baseline and will be updated by future work. For example, it may be possible to relate the number of waste packages available for incorporation to the energetics of the event.

Very dense particles cannot be transported significant distances by a convective column (from observations made with this model, "very dense" means "with density greater than about 5 g/cm^3 "). In these analyses, if the fuel fraction was greater than one then it was truncated to zero (to remove the contamination that these particles carry from the transport scenario). A fuel fraction of one corresponds to a contaminated particle composed of equal masses of fuel and volcanic ash. Since the average ash density is about 1.5 g/cm^3 and spent-fuel has an initial density of about 11 g/cm^3 , $FF(\rho^a) = 1$ roughly corresponds to a particle with a density of 5 g/cm^3 .

12/41

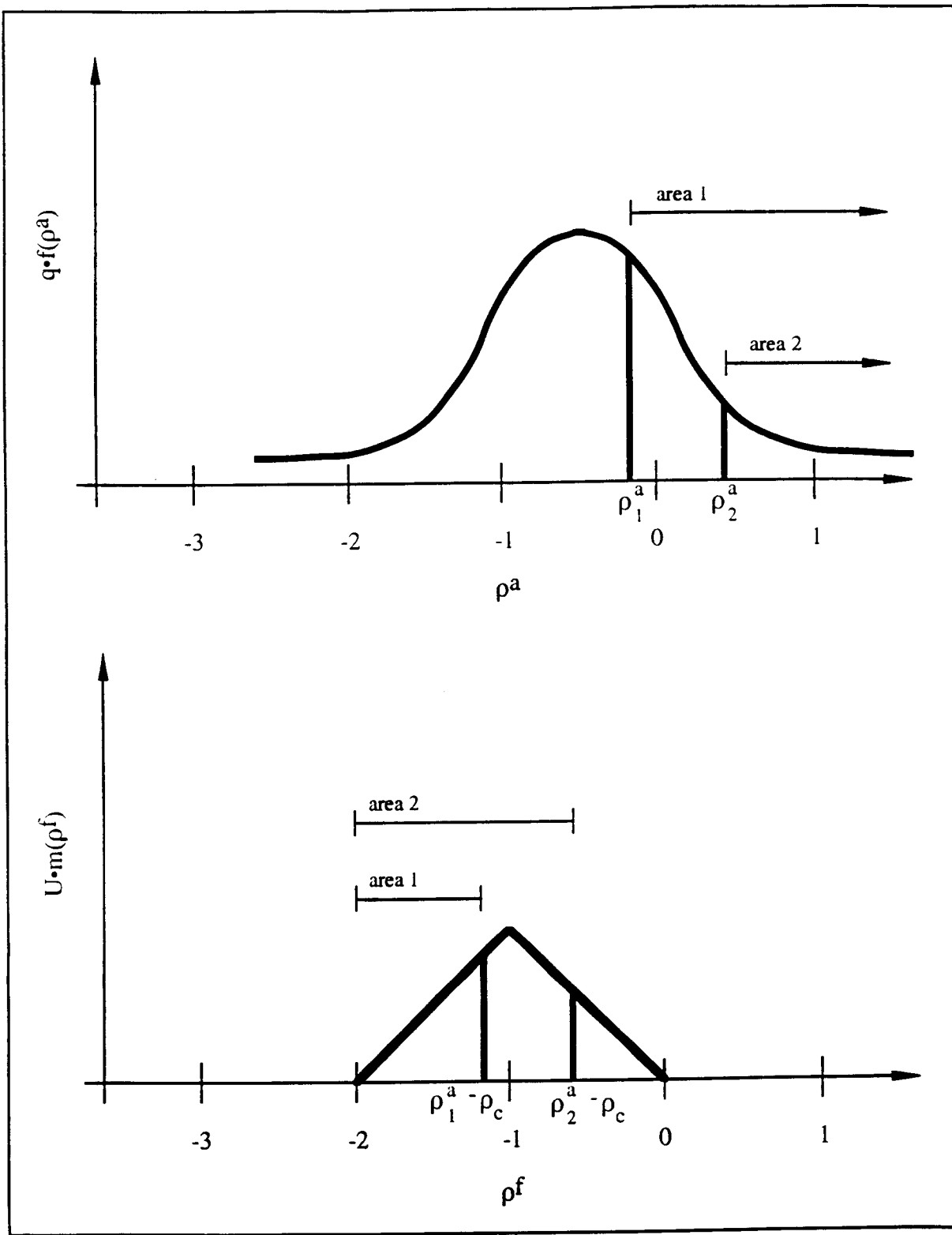


Figure 5. A diagram describing the fuel fraction as a function of ρ^a

To clarify this procedure further, consider the following simple, albeit unrealistic, example. Assume that the total quantity of volcanic ash released in the event (q) occurs in the following way: one-third of the volcanic ash mass has $\rho^a = -1$; one-third of the volcanic ash mass has $\rho^a = 0$; and one-third of the volcanic ash mass has $\rho^a = 1$. Assume that the total quantity of spent-fuel released in the event (U) occurs in the following: one-third of the fuel mass has $\rho^f = -2.01$; one-third of the fuel mass has $\rho^f = -1.01$; and one-third of the fuel mass has $\rho^f = -0.01$. For reasons previously stated, it is assumed that $\rho_c = 1$. For this simplistic example, it is only necessary to describe the fuel fraction at $\rho^a = -1, 0$ and 1 to completely describe the system.

The fuel fraction at these three values of ρ^a is given as follows:

$$FF(\rho^a = -1) = \frac{\frac{1}{3}U}{q} = \frac{1}{3} \frac{U}{q} \tag{2-8}$$

$$FF(\rho^a = 0) = \frac{\frac{1}{3}U}{q} + \frac{\frac{1}{3}U}{\frac{2}{3}q} = \frac{5}{6} \frac{U}{q} \tag{2-9}$$

$$FF(\rho^a = 1) = \frac{\frac{1}{3}U}{q} + \frac{\frac{1}{3}U}{\frac{2}{3}q} + \frac{\frac{1}{3}U}{\frac{1}{3}q} = \frac{11}{6} \frac{U}{q} \tag{2-10}$$

If it is assumed that U and q are equal then $FF(\rho^a = 1)$ is greater than 1, and hence its value must be truncated to zero because these particles are too dense to be transported significant distances by a convection column. Finally, the fuel fraction becomes:

14/41

$$\begin{aligned}
FF(\rho^a = -1) &= \frac{1}{3} \\
FF(\rho^a = 0) &= \frac{5}{6} \\
FF(\rho^a = 1) &= 0
\end{aligned}
\tag{2-11}$$

An isopleth map of the areal density of spent fuel as a function of position for a particular realization of the spent-fuel distribution is provided in Figure 6. The realization for which the spent-fuel contours are shown in Figure 6 occurred at a time of 829 yr. The sampled time of 829 yr is an arbitrary choice and any other event time within the TPI is equally as valid. Table 1 shows the radionuclide content of the spent-fuel at that point in time (in Ci/g of spent-fuel). The important simulation parameters that were sampled in the realization shown in Figure 6 are shown in Table 2, and the fuel fraction as a function of ρ^a for this case is shown in Figure 7. The volcanic parameters (and their interrelationships) that were held constant in these analyses are described in Jarzempa (1996). These parameters include such constants as the particle shape parameter, air viscosity and density, and particle terminal velocity at sea level. For a complete description of the parameters listed in Table 2 and the constant parameters and interrelationships, refer to Jarzempa (1996). In calculations presented in this report, radionuclide inventories have been determined by using the INVENT computer module described in Lozano et al., (1994). The time of event occurrence was sampled uniformly over the TPI with events occurring in the first 100 yr having zero dose to account for and active institutional controls for the first 100 yr after closure. During this initial period, controls would presumably prevent farming on the ash blanket. It was also assumed that the fuel had been aged 100 yr by repository closure to more accurately reflect the radionuclide inventory of the fuel.

2.5 DOSE CONVERSION

Conversion from radionuclide concentrations to dose was done using the GENII-S [Leigh et al. (1993)] code. Individual annual total effective dose equivalents (TEDEs) were calculated for each of 42 radionuclides for a resident Amargosa Desert farmer/rancher based upon unit radionuclide concentrations on the soil. The 42 radionuclides modeled in these calculations are as follows:

- Curium isotopes: 246, 245, 244, 243
- Americium isotopes: 243, 242m, 241
- Plutonium isotopes: 242, 241, 240, 239, 238
- Uranium isotopes: 238, 236, 235, 234, 233, 232
- Thorium isotopes: 230, 229
- Cesium isotopes: 137, 135
- Other isotopes: ^{237}Np , ^{231}Pa , ^{227}Ac , ^{226}Ra , ^{210}Pb , ^{151}Sm , ^{129}I , ^{126}Sn , $^{121\text{m}}\text{Sn}$, ^{107}Pd , ^{99}Tc , ^{94}Nb , ^{93}Mo , ^{93}Zr , ^{90}Sr , ^{79}Se , ^{63}Ni , ^{59}Ni , ^{36}Cl , ^{14}C

This list matches the one given in the Sandia TSPA-1993 [Wilson et al., (1994)], with one exception. That exception is $^{108\text{m}}\text{Ag}$, for which data to perform the dose conversion analyses was unavailable. In any case, this isotope is not expected to be a major contributor to dose. A Monte Carlo

15/41

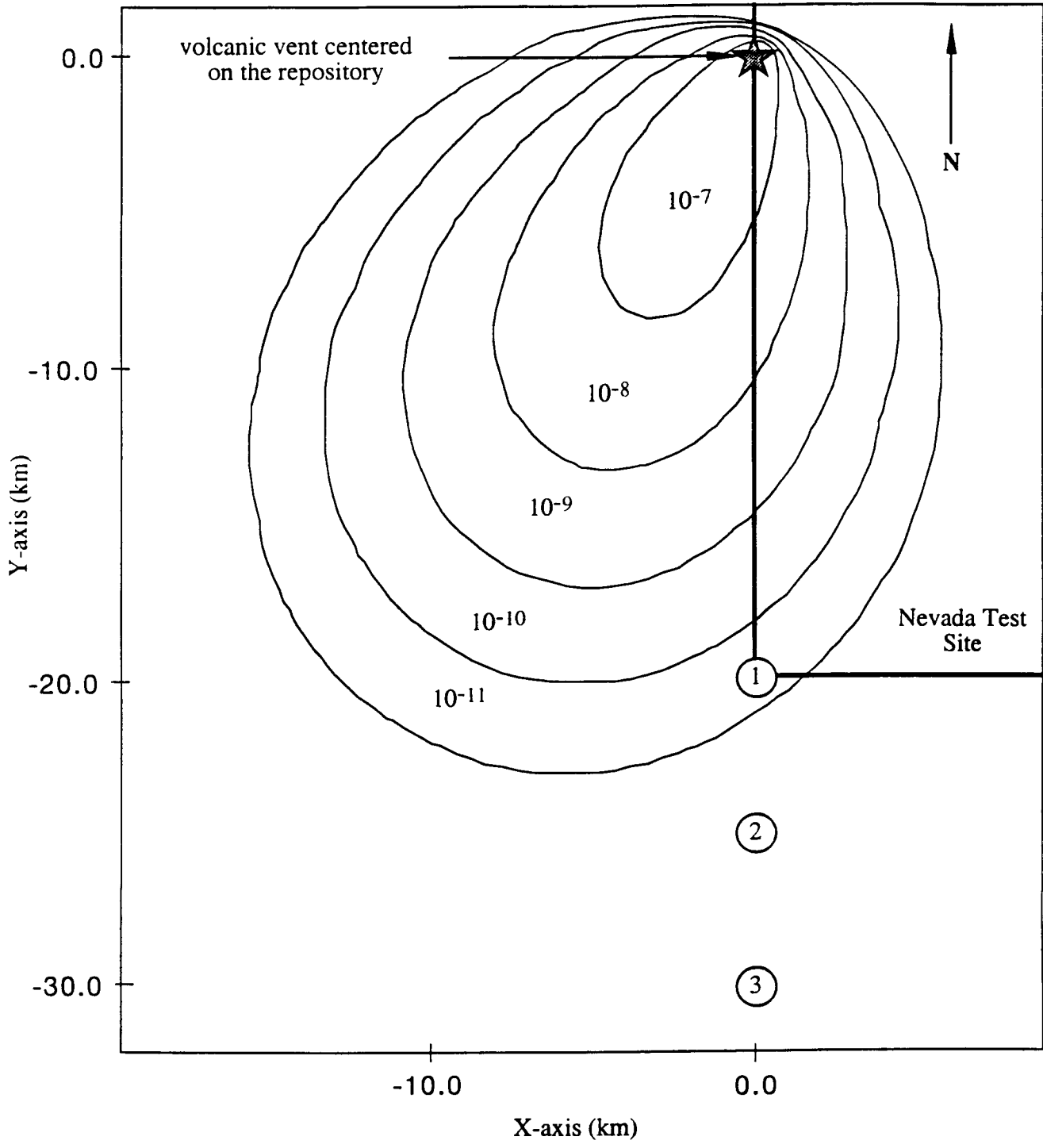


Figure 6. A spent-fuel isopleth map following an eruption with the parameters shown in Table 1. All densities shown are in g of spent-fuel/cm². In this particular realization, the event occurred at t=829 yr.

16/41

Table 1. Radionuclide concentration in the spent-fuel in curies per gram of spent-fuel for the realization shown in Figure 6

Radionuclide	Ci of radionuclide per g of spent fuel
Ac-227	3.00E-10
Am-241	1.10E-03
Am-242m	1.80E-07
Am-243	1.40E-05
C-14	1.20E-06
Cl-36	1.20E-08
Cm-243	3.40E-14
Cm-244	2.80E-17
Cm-245	1.20E-07
Cm-246	2.30E-08
Cs-135	3.50E-07
Cs-137	4.60E-10
I-129	2.90E-08
Mo-93	8.60E-09
Nb-94	4.90E-07
Ni-59	2.40E-06
Ni-63	6.40E-07
Np-237	8.90E-07
Pa-231	3.20E-10
Pb-210	2.00E-09
Pd-107	1.00E-07
Pu-238	3.30E-06
Pu-239	3.00E-04
Pu-240	4.70E-04
Pu-241	1.20E-07
Pu-242	1.60E-06
Ra-226	2.10E-09
Se-79	3.80E-07
Sm-151	5.80E-07
Sn-121m	9.20E-12
Sn-126	7.10E-07
Sr-90	1.80E-10
Tc-99	1.20E-05
Th-229	7.80E-11
Th-230	1.40E-08
U-232	9.30E-12
U-233	2.40E-09
U-234	1.90E-06
U-235	1.70E-08
U-236	2.50E-07
U-238	3.20E-07
Zr-93	1.80E-06

17/41

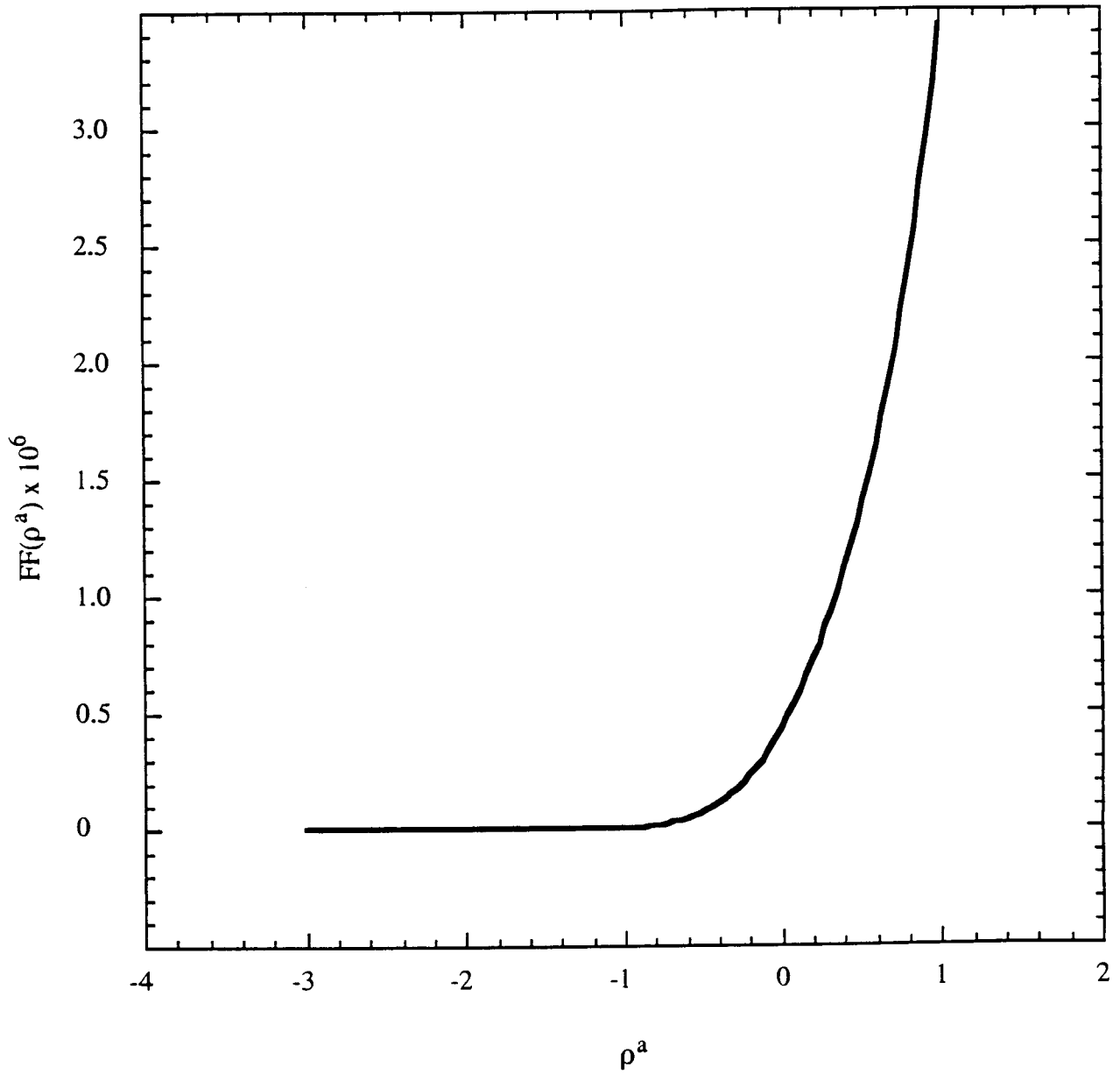


Figure 7. A plot of the normalized fuel fraction as a function of ρ^a for the realization shown in Figure 6.

18/41

Table 2. Listing of the sampled parameters for the realization shown in Figure 6

Parameter	Distribution Type	Range	Sampled Value
Total volcanic ash mass (g)	see Jarzempa (1996)		3.73×10^{13}
Event duration (s)	Loguniform	[3.25, 6.83]	3.3×10^4
Event power (W)	Lognormal	[0. 13.8]	8.23×10^{11}
Column height (km)	function of power		7.809
Mean particle diameter (cm)	Logtriangular	[-2, 1]	0.068
Standard deviation of particle log-diameter	Loguniform	[-3, 0.3]	0.995
Beta ¹	Loguniform	[0.01, 0.5]	0.305
Wind speed (cm/s)	Exponential		832.4
Wind direction (degrees-relation to due east)	see Jarzempa (1996)		-112.5
Mass of fuel ejected (g)	Constant		1.0×10^7

¹ Beta is a constant controlling particle diffusion in the eruption column.

style analysis with 125 realizations is used to generate TEDE distributions. Input parameter values were sampled from distributions using Latin Hypercube Sampling. Tables 3 through 6 present the results as the expected values and standard deviations of annual TEDE distributions for each pathway calculated for each radionuclide assuming that the radionuclides were deposited on the surface of the soil with unit concentration. Table 7 gives the total pathway DCFs assuming that the individual consumes 50 percent of his food from contaminated sources.

2.6 CALCULATION OF THE EXPECTED VALUE OF THE PEAK DOSE TO THE AMARGOSA DESERT FARMER/RANCHER IN THE TIME PERIOD OF INTEREST

Values of the peak annual effective dose equivalent (hereafter called dose) to the Amargosa Desert farmer/rancher in the TPI for each realization were calculated for TPIs of 10,000 yr and 1,000,000 yr. For each TPI, 1,000 dose realizations were obtained. The dose to the farmer/rancher was calculated based on the dose conversion factors in the previous section. The expected value of the peak dose in the TPI to the farmer/rancher is given by:

$$E(\dot{D}, TPI) = p(TPI) \sum_{n=1}^{N_R} \frac{1}{N_R} \cdot \dot{D}(n) \tag{2-12}$$

19/41

Table 3. Dose Conversion Factors (DCFs) for the animal product ingestion pathway

Radionuclide	Expected value of the DCF [rem/yr/Ci/cm ²]	Standard Deviation [rem/yr/Ci/cm ²]
Ac-227	1.70E+08	1.40E+08
Am-241	3.10E+07	2.40E+07
Am-242m	3.00E+07	2.30E+07
Am-243	3.10E+07	2.40E+07
C-14	0.00E+00	0.00E+00
Cl-36	2.70E+08	2.20E+08
Cm-243	1.50E+07	1.50E+07
Cm-244	1.20E+07	1.20E+07
Cm-245	2.30E+07	2.10E+07
Cm-246	2.30E+07	2.20E+07
Cs-135	8.50E+07	6.50E+07
Cs-137	5.90E+08	4.50E+08
I-129	2.70E+09	2.10E+09
Mo-93	1.10E+06	9.50E+05
Nb-94	1.30E+03	1.10E+03
Ni-59	1.10E+06	1.00E+06
Ni-63	3.10E+06	2.70E+06
Np-237	1.10E+09	8.30E+08
Pa-231	3.60E+07	2.80E+07
Pb-210	1.00E+09	8.00E+08
Pd-107	5.40E+05	4.80E+05
Pu-238	1.10E+05	8.70E+04
Pu-239	1.20E+05	8.80E+04
Pu-240	1.20E+05	8.80E+04
Pu-241	4.40E+03	3.40E+03
Pu-242	1.10E+05	8.30E+04
Ra-226	5.00E+08	3.00E+08
Se-79	3.50E+07	2.60E+07
Sm-151	3.90E+05	3.00E+05
Sn-121m	3.60E+07	2.80E+07
Sn-126	3.40E+08	2.60E+08
Sr-90	3.60E+08	2.60E+08
Tc-99	1.50E+06	1.20E+06
Th-229	5.30E+07	4.70E+07
Th-230	1.40E+06	1.10E+06
U-232	1.30E+07	1.10E+07
U-233	4.50E+06	3.70E+06
U-234	1.10E+05	3.70E+06
U-235	4.60E+06	3.90E+06
U-236	4.10E+06	3.50E+06
U-238	4.40E+06	3.60E+06
Zr-93	6.00E+02	4.70E+02

20/41

Table 4. Dose Conversion Factors (DCFs) of the terrestrial food ingestion pathway

Radionuclide	Expected value of the DCF [rem/yr/Ci/cm ²]	Standard Deviation [rem/yr/Ci/cm ²]
Ac-227	2.70E+10	1.70E+10
Am-241	6.90E+09	4.40E+09
Am-242m	6.70E+09	4.20E+09
Am-243	6.90E+09	4.40E+09
C-14	0.00E+00	0.00E+00
Cl-36	4.10E+08	2.50E+08
Cm-243	4.80E+09	3.00E+09
Cm-244	3.80E+09	2.40E+09
Cm-245	7.10E+09	4.50E+09
Cm-246	7.20E+09	4.50E+09
Cs-135	1.40E+07	8.30E+06
Cs-137	9.50E+07	5.80E+07
I-129	4.90E+08	3.00E+08
Mo-93	4.80E+06	2.20E+06
Nb-94	1.40E+07	8.80E+06
Ni-59	4.00E+05	2.50E+05
Ni-63	1.10E+06	6.70E+05
Np-237	1.00E+10	6.40E+09
Pa-231	2.10E+10	1.30E+10
Pb-210	1.10E+10	6.70E+09
Pd-107	3.30E+05	1.90E+05
Pu-238	8.34E+07	5.28E+07
Pu-239	9.50E+07	6.00E+07
Pu-240	9.60E+07	6.00E+07
Pu-241	2.30E+06	1.50E+06
Pu-242	9.00E+07	5.70E+07
Ra-226	1.90E+09	1.20E+09
Se-79	1.60E+07	1.00E+07
Sm-151	7.30E+05	4.60E+05
Sn-121m	4.30E+06	2.70E+06
Sn-126	4.00E+07	2.50E+07
Sr-90	3.70E+08	1.90E+08
Tc-99	4.40E+07	2.60E+07
Th-229	7.10E+09	4.50E+09
Th-230	1.00E+09	6.50E+08
U-232	1.60E+08	1.00E+08
U-233	5.10E+07	3.20E+07
U-234	5.00E+07	3.10E+07
U-235	5.40E+07	3.40E+07
U-236	4.70E+07	2.90E+07
U-238	5.90E+07	3.70E+07
Zr-93	3.10E+06	2.00E+06

2/41

Table 5. Dose Conversion Factors (DCFs) for the external radiation pathway

Radionuclide	Expected value of the DCF [rem/yr/Ci/cm ²]	Standard Deviation [rem/yr/Ci/cm ²]
Ac-227	1.40E+05	7.70E+03
Am-241	4.60E+07	2.60E+06
Am-242m	2.60E+06	1.50E+05
Am-243	4.60E+07	2.60E+06
C-14	1.40E+04	7.90E+02
Cl-36	5.90E+05	3.30E+04
Cm-243	1.10E+08	6.20E+06
Cm-244	7.80E+05	4.40E+04
Cm-245	7.60E+07	4.30E+06
Cm-246	6.90E+05	3.90E+04
Cs-135	3.00E+04	1.70E+03
Cs-137	4.80E+08	2.70E+07
I-129	2.20E+07	1.30E+06
Mo-93	4.60E+06	2.60E+05
Nb-94	1.30E+09	7.50E+07
Ni-59	0.00E+00	0.00E+00
Ni-63	0.00E+00	0.00E+00
Np-237	2.60E+07	1.50E+06
Pa-231	3.50E+07	2.00E+06
Pb-210	2.20E+06	1.30E+05
Pd-107	0.00E+00	0.00E+00
Pu-238	5.47E+05	3.06E+04
Pu-239	3.20E+05	1.80E+04
Pu-240	7.00E+05	4.00E+04
Pu-241	1.70E+03	1.10E+04
Pu-242	5.90E+05	3.30E+04
Ra-226	5.60E+06	3.10E+05
Se-79	1.80E+04	1.00E+03
Sm-151	4.40E+03	2.50E+02
Sn-121m	4.30E+06	2.40E+05
Sn-126	4.80E+07	2.70E+06
Sr-90	2.40E+05	1.40E+04
Tc-99	6.90E+04	3.90E+03
Th-229	7.40E+07	4.20E+06
Th-230	6.50E+05	3.70E+04
U-232	8.90E+05	5.50E+04
U-233	6.30E+05	3.50E+04
U-234	6.50E+05	3.70E+04
U-235	1.30E+08	7.30E+06
U-236	5.70E+05	3.20E+04
U-238	4.80E+05	2.70E+04
Zr-93	0.00E+00	0.00E+00

22/41

Table 6. Dose Conversion Factors (DCFs) for the inhalation from resuspension pathway

Radionuclide	Expected value of the DCF [rem/yr/Ci/cm ²]	Standard Deviation [rem/yr/Ci/cm ²]
Ac-227	2.10E+07	2.70E+06
Am-241	7.00E+06	9.10E+05
Am-242m	6.70E+06	8.60E+05
Am-243	7.00E+06	9.10E+05
C-14	3.30E+01	4.20E+00
Cl-36	3.50E+01	4.50E+00
Cm-243	4.90E+06	6.30E+05
Cm-244	3.90E+06	5.10E+05
Cm-245	7.10E+06	9.30E+05
Cm-246	7.20E+06	9.30E+05
Cs-135	7.10E+01	9.20E+00
Cs-137	4.70E+02	6.20E+01
I-129	2.40E+03	3.10E+02
Mo-93	1.60E+01	2.10E+00
Nb-94	6.00E+03	7.80E+02
Ni-59	1.40E+01	1.80E+00
Ni-63	3.50E+01	4.60E+00
Np-237	1.00E+07	1.30E+06
Pa-231	1.40E+07	1.80E+06
Pb-210	2.10E+05	2.80E+04
Pd-107	2.20E+02	2.60E+01
Pu-238	4.26E+06	5.56E+05
Pu-239	4.80E+06	6.20E+05
Pu-240	4.80E+06	6.20E+05
Pu-241	7.80E+04	1.00E+04
Pu-242	4.60E+06	6.00E+05
Ra-226	1.30E+05	1.70E+04
Se-79	1.50E+02	2.00E+01
Sm-151	4.70E+02	6.20E+01
Sn-121m	1.80E+02	2.30E+01
Sn-126	1.50E+03	2.00E+02
Sr-90	3.20E+03	4.20E+02
Tc-99	1.40E+02	1.80E+01
Th-229	2.70E+07	3.50E+06
Th-230	4.10E+06	5.30E+05
U-232	1.00E+07	1.40E+06
U-233	2.10E+06	2.80E+05
U-234	2.10E+06	2.70E+05
U-235	2.00E+06	2.50E+05
U-236	2.00E+06	2.60E+05
U-238	1.90E+06	2.40E+05
Zr-93	1.30E+03	1.70E+02

Table 7. Total pathway Dose Conversion Factors (DCFs)

Radionuclide	Expected value of the DCF [rem/yr/Ci/cm ²]	Standard Deviation [rem/yr/Ci/cm ²]
Ac-227	1.36E+10	1.70E+10
Am-241	3.52E+09	4.40E+09
Am-242m	3.37E+09	4.20E+09
Am-243	3.52E+09	4.40E+09
C-14	1.40E+04	7.90E+02
Cl-36	3.41E+08	3.33E+08
Cm-243	2.52E+09	3.00E+09
Cm-244	1.91E+09	2.40E+09
Cm-245	3.64E+09	4.50E+09
Cm-246	3.62E+09	4.50E+09
Cs-135	4.95E+07	6.55E+07
Cs-137	8.23E+08	4.55E+08
I-129	1.62E+09	2.12E+09
Mo-93	7.55E+06	2.41E+06
Nb-94	1.31E+09	7.55E+07
Ni-59	7.50E+05	1.03E+06
Ni-63	2.10E+06	2.78E+06
Np-237	5.59E+09	6.45E+09
Pa-231	1.06E+10	1.30E+10
Pb-210	6.00E+09	6.75E+09
Pd-107	4.35E+05	5.16E+05
Pu-238	4.66E+07	5.28E+07
Pu-239	5.27E+07	6.00E+07
Pu-240	5.36E+07	6.00E+07
Pu-241	1.23E+06	1.50E+06
Pu-242	5.02E+07	5.70E+07
Ra-226	1.21E+09	1.24E+09
Se-79	2.55E+07	2.79E+07
Sm-151	5.65E+05	5.49E+05
Sn-121m	2.45E+07	2.81E+07
Sn-126	2.38E+08	2.61E+08
Sr-90	3.65E+08	3.22E+08
Tc-99	2.28E+07	2.60E+07
Th-229	3.68E+09	4.50E+09
Th-230	5.05E+08	6.50E+08
U-232	9.74E+07	1.01E+08
U-233	3.05E+07	3.22E+07
U-234	2.78E+07	3.12E+07
U-235	1.61E+08	3.50E+07
U-236	2.81E+07	2.92E+07
U-238	3.41E+07	3.72E+07
Zr-93	1.55E+06	2.00E+06

24/41

where:

- $\dot{D}(n)$ = the peak dose to the farmer/rancher in the TPI for realization n
- N_R = the number of event realizations

The quantity $\dot{D}(n)$ is calculated as:

$$\dot{D}(n) = \sum_{i=1}^{42} {}^T DCF_i \cdot C_i \quad (2-13)$$

where:

- ${}^T DCF_i$ = the total pathway DCF for radionuclide i (Table 7)
- C_i = the radionuclide surficial concentration at the dose point

The expected doses generated by Equation (2-12) assume that the only scenario for delivering doses to the farmer/rancher is extrusive volcanism. The summation in Equation (2-12) represents the expected value of the dose given that an extrusive event occurs in the TPI within the repository zone and disrupts one waste package containing 10 Metric Tonnes of Uranium (MTU) of spent-fuel. By multiplying the summation by the probability of the event occurring in the TPI, the overall expected value was obtained.

Table 8 shows the expected value of the peak annual effective dose equivalent in the TPI as a function of position of the dose point on the earth's surface. The x - y coordinate axis is oriented with positive x in the due east direction, the positive y in the due north direction and is centered on the repository. Appendix A shows the Complementary Cumulative Distribution Functions (CCDFs) and the stack histograms of the common logarithm of the doses for the 1,000 realizations for each of the positions and TPIs shown in Table 8.

2.7 RESULTS

The results show a generally decreasing dose with distance from the event (Table 8). The CCDFs and the stack histogram of doses for the three dose points and two TPIs are given in Appendix A. These results indicate that increasing the TPI from 10,000 yr to 1,000,000 yr generally increases the expected value of the peak doses in the TPI by a factor of two to four, although the magnitude of this increase is somewhat uncertain due to the large standard deviation on the estimates. Increase in the importance of volcanism is more pronounced when one compares the low dose rate ranges of the CCDFs for the two TPIs for the same dose point, as shown in Appendix A. The differences in the high dose rate ranges in the CCDFs are an artifact of the sampling scheme. Since 1,000 realizations were achieved for each TPI, the 10,000 yr TPI case has proportionately more realizations at times when the waste is more hazardous, thus a more accurate estimate of the "maximum hazard" of the exposure scenario is achieved. Results affirm that by merely increasing the TPI, the importance of low probability, high consequence events such as volcanism has significantly increased when compared with scenarios that are certain to occur such as an undisturbed repository leaching small amounts of radionuclides to the water table with subsequent drinking water pathway doses. These analyses assumed that 10 MTU (one waste package) of

25/41

Table 8. Expected values and standard deviations as a function of position and the time period of interest

Dose Point Number	Period of Interest (yr)	Dose Point Location		Expected Annual Effective Dose Equivalent (rem/yr)	Standard Deviation (rem/yr)
		x (km)	y (km)		
1	10,000	0	-20	2.7×10^{-6}	2.2×10^{-3}
2	10,000	0	-25	7.5×10^{-7}	7.6×10^{-4}
3	10,000	0	-30	2.5×10^{-7}	3.4×10^{-4}
1	1,000,000	0	-20	7.7×10^{-6}	6.1×10^{-4}
2	1,000,000	0	-25	1.8×10^{-6}	1.4×10^{-4}
3	1,000,000	0	-30	4.4×10^{-7}	4.1×10^{-5}

spent-fuel is incorporated in the volcanic ash ejected during the event. This assumption can be updated as more information becomes available. Future models may couple the amount of spent-fuel ejected with the energetics of the event.

3 ASSUMPTIONS AND LIMITATIONS

3.1 ASSUMPTIONS

The following assumptions have been made in the calculations described in this report:

- The volcanic ash dispersal model and parameter ranges described in Jarzempa (1996) are valid for modeling volcanic ash dispersals at YM
- The doses are calculated for an Amargosa Desert farmer/rancher as described in LaPlante et al. (1995) with all of the associated assumptions and limitations
- The selected dose points describe the possible locations of the critical group
- Variances in the DCF are small compared with other parameter variances in the calculation, hence the mean values for DCFs can be used without greatly affecting the expected doses
- Volcanic ash particles carry only spent-fuel particles less than or equal to one-tenth of the volcanic ash particle diameter

- Consistent with the above assumption, a contaminated particle can have no more than one-half its mass comprised of spent-fuel
- One waste package container (10 MTU of fuel) is available for incorporation in each event
- The farmer/rancher receives 50 percent of beef, milk, fruit, grains, and vegetables from contaminated sources.

3.2 SUGGESTIONS FOR FUTURE WORK

- Incorporate resuspension factors and “soil” properties of volcanic ash into the analyses
- Incorporate time dependent spent-fuel particle size distributions into the analyses
- Investigate waste package performance under exposure to magma at the aforementioned conditions
- Investigate the relationship between the volcanic event magnitude and the number of waste packages available for incorporation
- Investigate the sensitivity of the analyses to the parameter ρ_c .

4 SUMMARY/CONCLUSIONS

The annual effective dose equivalents calculated from the analyses described in this report were based on the volcanic ash dispersion model described in Jarzempa (1996). In addition, improvements to this model have been made to more realistically model the distribution of spent-fuel within the extruded particulate matter. Expected peak dose calculations to an Amaragosa Desert farmer/rancher were made assuming a lifestyle as described by LaPlante et al. (1995) and for different locations of this individual on the earth’s surface after the event. The analyses in this report show that increasing the TPI has the effect of increasing the importance of low probability, high consequence events, such as extrusive volcanism, when compared with scenarios that are certain to occur regardless of the TPI (e.g., undisturbed repository).

5 REFERENCES

Anspaugh, L.R., J.H. Shinn, P.L. Phelps, and N.C. Kennedy. 1975. Resuspension and redistribution of plutonium in soils. *Health Physics* 29: 571-582.

Anspaugh, L.R. 1987. *Retention by Vegetation of Radionuclides Deposited in Rainfall—A Literature Summary*. UCRL-53810. Livermore, CA: Lawrence Livermore National Laboratory.

Baes, C.F. III, R.D. Sharp, A.L. Sjoreen, and R.W. Shor. 1982. *A Review and Analysis of Parameters for Assessing Transport of Environmentally Released Radionuclides through Agriculture*. ORNL-5786. Oak Ridge, TN: Oak Ridge National Laboratories.

- Breshears, D.D., T.B. Kirchner, M.D. Otis, and F.W. Whicker. 1989. Uncertainty in predictions of fallout radionuclides in foods and of subsequent ingestion. *Health Physics* 57(6): 943-953.
- Breshears, D.D., T.B. Kirchner, and F.W. Whicker. 1992. Contaminant transport through agroecosystems: Assessing relative importance of environmental, physiological, and management factors. *Ecological Applications* 2(3): 285-297.
- Clark, P.A.E., et al. 1985. *Post Irradiation Examination of Two High Burnup Fuel Rods Irradiated in the Halden BWR*. AEREG 3207. AERE Harwell Report.
- Connor, C.B., and B.E. Hill. 1995. Three Nonhomogeneous Poisson Models for the Probability of Basaltic Volcanism. *Journal of Geophysical Research* 100(10): 10,107-10,125.
- Eckerman, K.F., and J.C. Ryman. 1993. *External Exposure to Radionuclides in Air, Water, and Soil: Exposure-to-Dose Coefficients for General Application, Based on the 1987 Federal Radiation Protection Guidance*. Federal Guidance Report No. 12. Oak Ridge, TN: Oak Ridge National Laboratory.
- Hoffman, F.O., R.H. Gardner, and K.F. Eckerman. 1982. *Variability in Dose Estimates Associated with the Food Chain Transport and Ingestion of Selected Radionuclides*. NUREG/CR-2612. Oak Ridge, TN: Oak Ridge National Laboratory.
- ICRP [International Council for Radiation Protection]. 1977. *Recommendations of the ICRP*. ICRP Publication 26: 1(3): Pergamon Press. Oxford, UK.
- ICRP [International Council for Radiation Protection]. 1985. *Principles of Monitoring for the Radiation Protection of the Population*. ICRP Publication 43: 15(1): Pergamon Press. Oxford, UK.
- ICRP [International Council for Radiation Protection]. 1991. *Radiation Protection, 1990 Recommendations of International Commission on Radiological Protection*. ICRP Publication 60. Annals of the ICRP. Oxford, UK.
- International Atomic Energy Agency. 1994. *Handbook of Parameter Values for the Prediction of Radionuclide Transfer in Temperate Environments*. Technical Report Series No. 364. Vienna, Austria: International Atomic Energy Agency.
- Jarzemba, M.S. 1996. Stochastic Radionuclide Distributions after a Basaltic Eruption for Performance Assessments of Yucca Mountain. Submitted for publication in *Nuclear Technology*.
- Kennedy, W.E., and D.L. Strenge. 1992. *Residual Radioactive Contamination from Decommissioning: Technical Basis for Translating Contamination Levels to Annual Total Effective Dose Equivalent*. NUREG/CR-5512, Vol. 1. Richland, WA: Pacific Northwest Laboratory.

- LaPlante, P.A., S.J. Maheras, and M.S. Jarzempa. 1995. *Initial Analyses of Site-Specific Dose Assessment Parameters and Exposure Pathways Applicable to a Groundwater Release Scenario at Yucca Mountain*. CNWRA 95-018. San Antonio, TX: Center for Nuclear Waste Regulatory Analyses.
- Leigh, C.D., B.M. Thompson, J.E. Campbell, D.E. Longsine, R.A. Kennedy, et al. 1993. *User's Guide for GENI-S: A Code for Statistical and Deterministic Simulation of Radiation Doses to Humans from Radionuclides in the Environment*. SAND 91-0561. Albuquerque, NM: Sandia National Laboratories.
- Lozano, A.S., H. Karimi, J.P. Cornelius, R.D. Manteufel, and R.W. Janetzke. 1994. *INVENT: A Module for the Calculation of Radionuclide Inventories, Software Description, and User's Guide*. CNWRA 94-016. San Antonio, TX: Center for Nuclear Waste Regulatory Analyses.
- Nevada Division of Water Resources. 1995. *Preliminary Summary of Ground Water Pumpage Inventory for Amargosa Valley Basin No. 230 from 1989 through 1993*. Carson City, NV: Nevada Division of Water Resources. Unpublished.
- Nevada Agricultural Statistics Service. 1988. *Nevada Agricultural Statistics: 1, 1987-88*. Reno, NV: Nevada Agricultural Statistics Service.
- Otis, M.D. 1983. *Sensitivity and Uncertainty Analysis of the PATHWAY Radionuclide Transport Model*. Ph.D. Dissertation. Fort Collins, CO: Colorado State University.
- Suzuki, T. 1983. A theoretical model for dispersion of tephra. *Arc Volcanism: Physics and Tectonics*. Tokyo: Terra Scientific Publishing: 95-113.
- U.S. Department of Commerce. 1989. *Census of Agriculture, Volume 1: Geographic Area Series, Part 28: Nevada State and County Data*. AC87-A-28. Washington DC: U.S. Department of Commerce.
- Walker, G.P.L., L. Wilson, and E.L.G. Bowell. 1970. Explosive Volcanic Eruptions-I: The Rate of Fall of Pyroclasts. *Geophysical Journal of the Royal Astrological Society* 22: 377-383.
- Wescott, R.G., M.P. Lee, N.A. Eisenberg, and R.G. Baca (Eds.). 1995. *NRC Iterative Performance Assessment, Phase 2*. NUREG 1464. Washington, DC: Nuclear Regulatory Commission.
- Wilson, M., J.H. Gauthier, R.W. Barnard, G.E. Barr et al. 1994. *Total System Performance Assessment for Yucca Mountain SNL Second Iteration (TSPA-1993)*. SAND 93-2675. Albuquerque, NM: Sandia National Laboratories.
- Yu, C., A.J. Zielen, J.J. Cheng, and Y.C. Yuan. 1993. *Manual for Implementing Residual Radioactive Material Guidelines Using RESRAD, Version 5.0*. ANAL/EAD/LD-2. Argonne, IL: Argonne National Laboratory

29/41

APPENDIX A

30/4/1

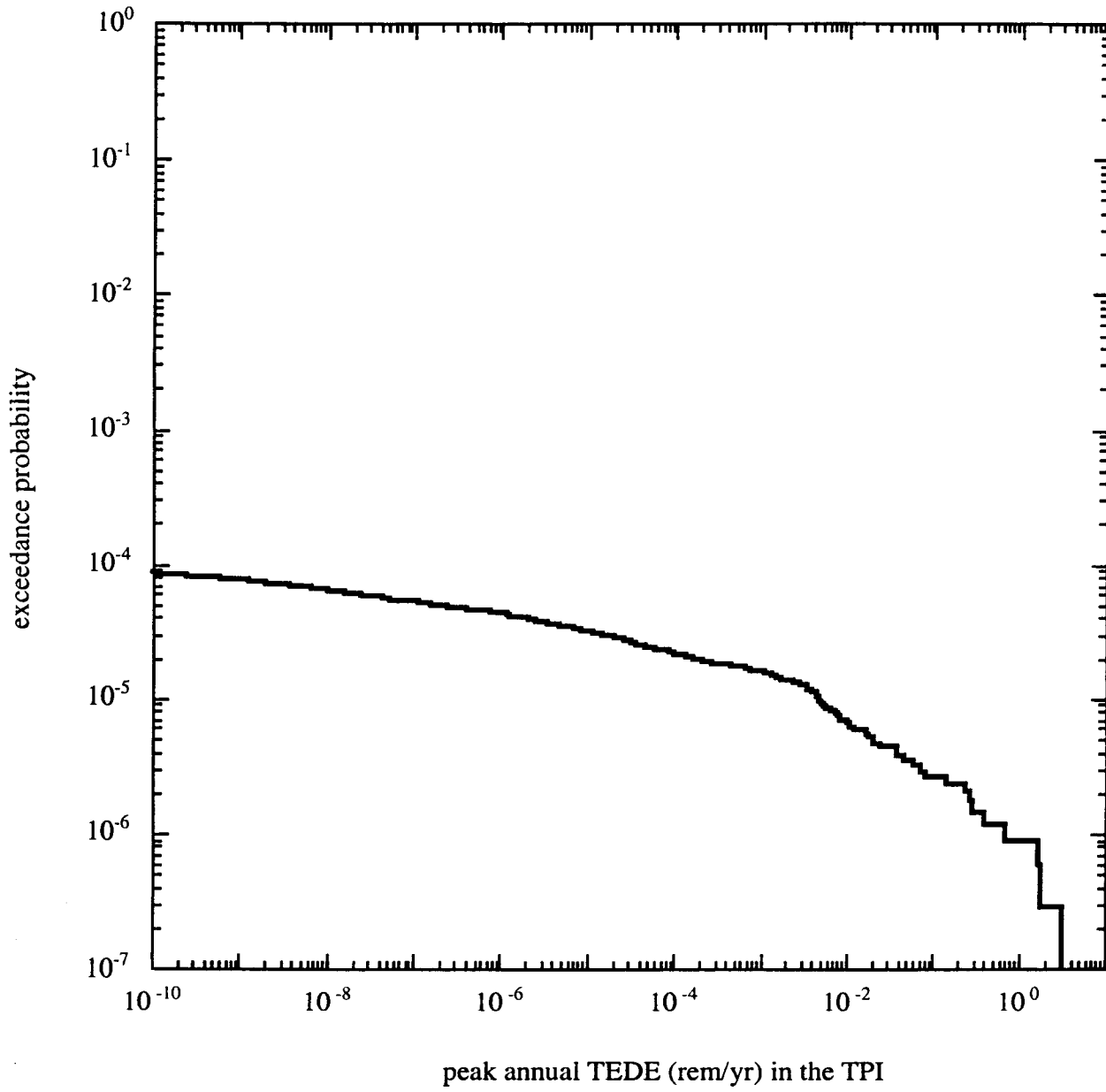


Figure A-1. The CCDF of the peak annual TEDE (rem/yr) at dose point 1 for a TPI of 10,000 yr .

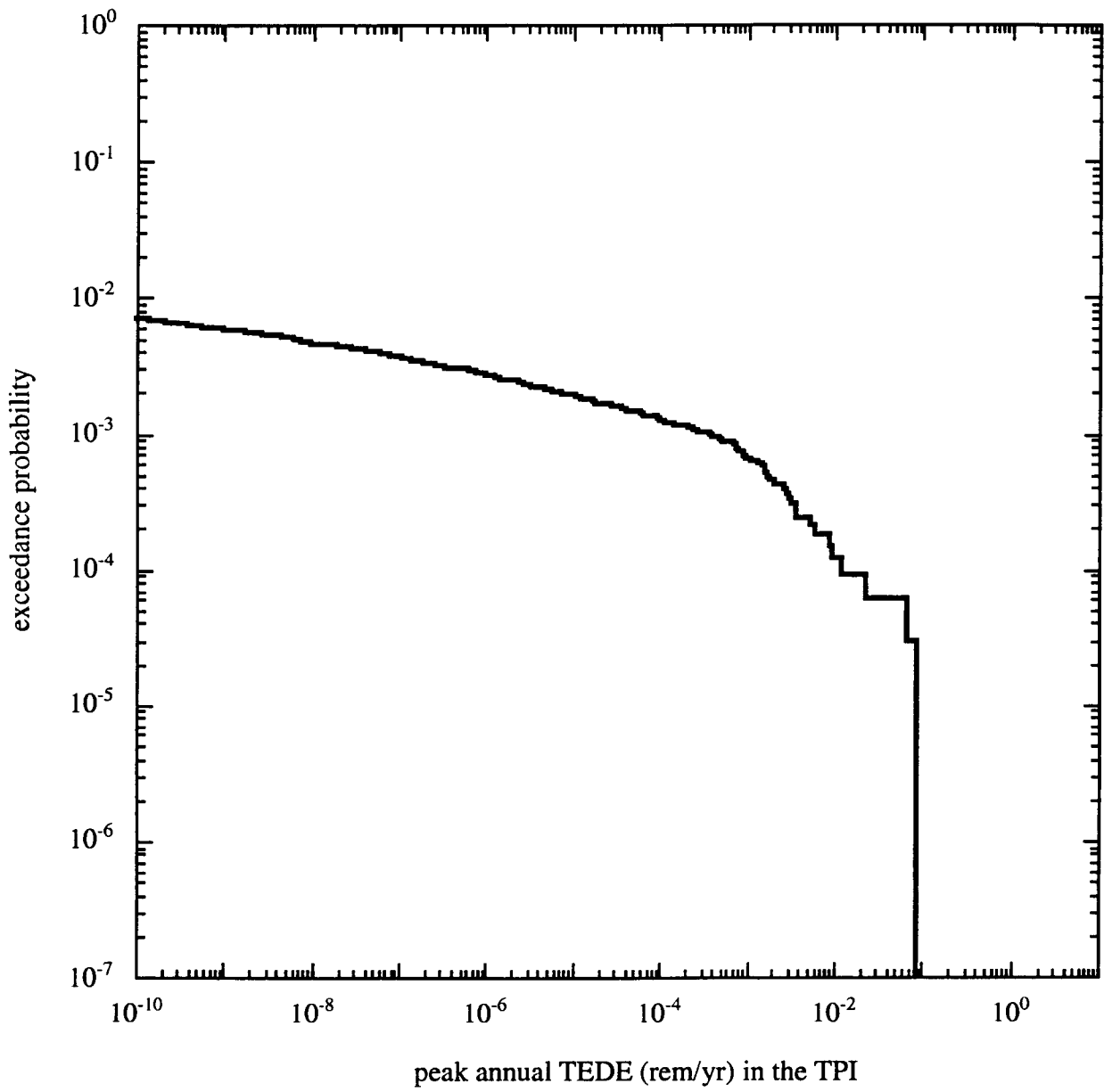


Figure A-2. The CCDF of the peak annual TEDE (rem/yr) at dose point 1 for a TPI of 1,000,000 yr

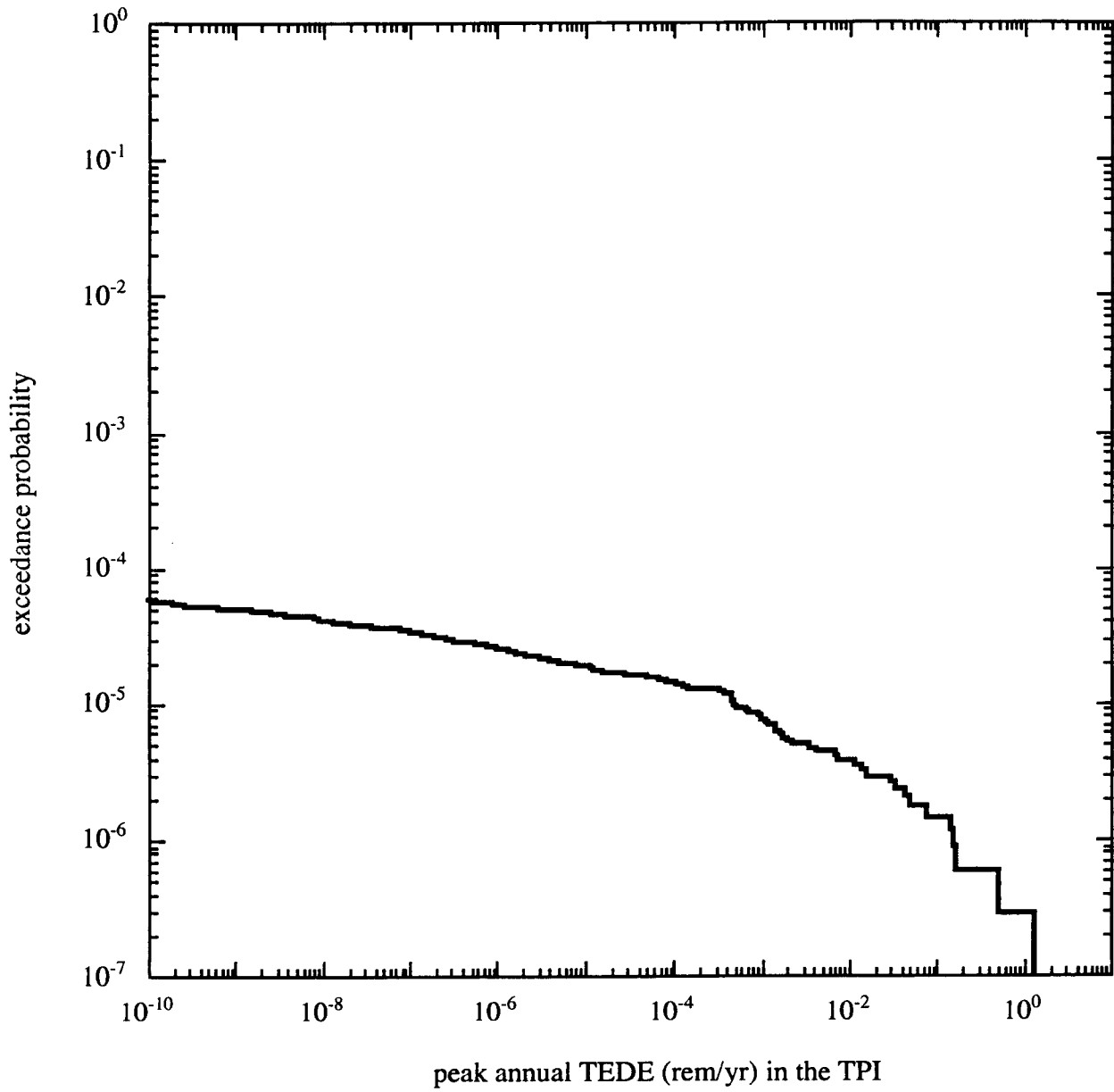


Figure A-3. The CCDF of the peak annual TEDE (rem/yr) at dose point 2 for a TPI of 10,000 yr

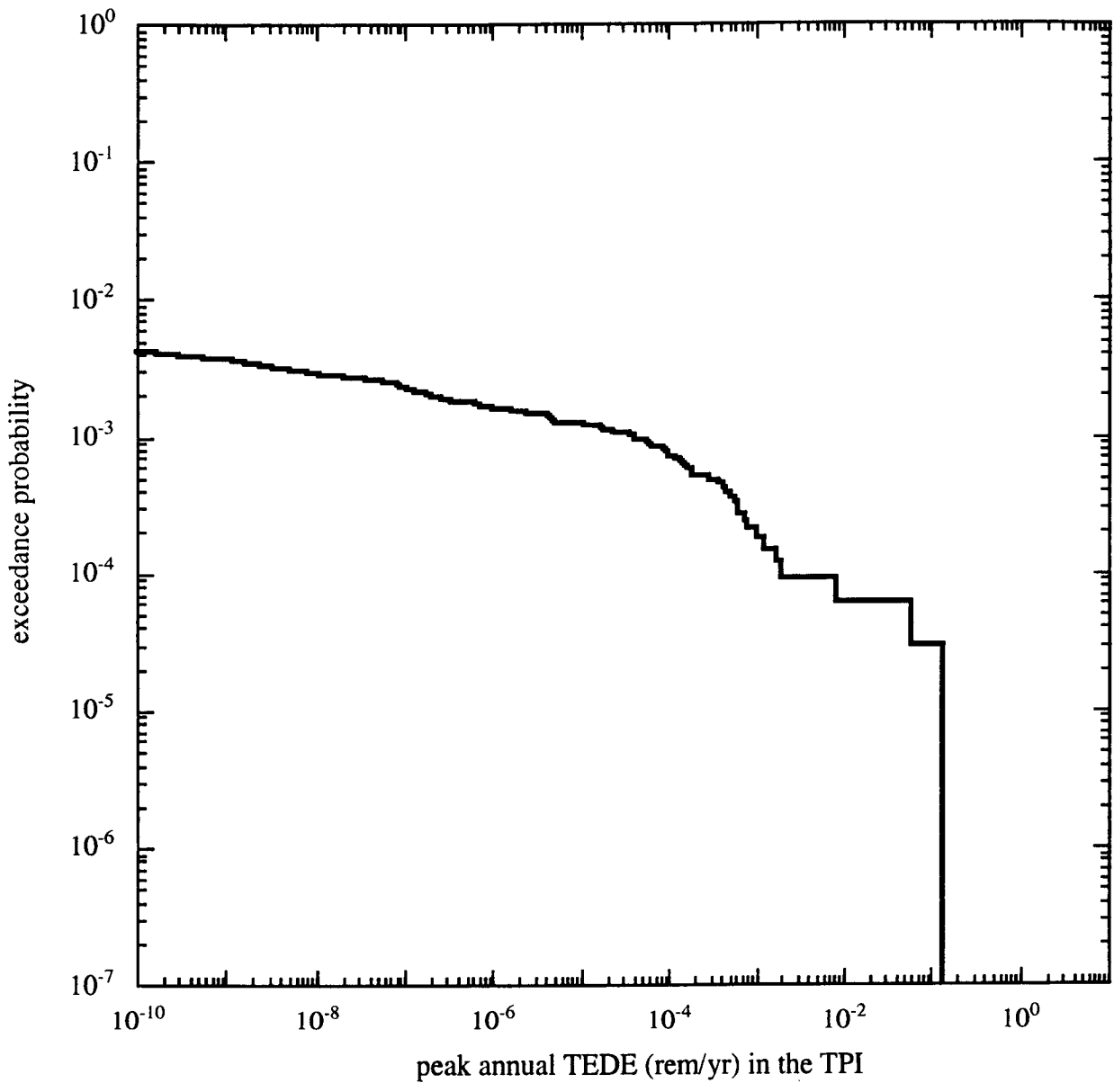


Figure A-4. The CCDF of the peak annual TEDE (rem/yr) at dose point 2 for a TPI of 1,000,000 yr

34/41

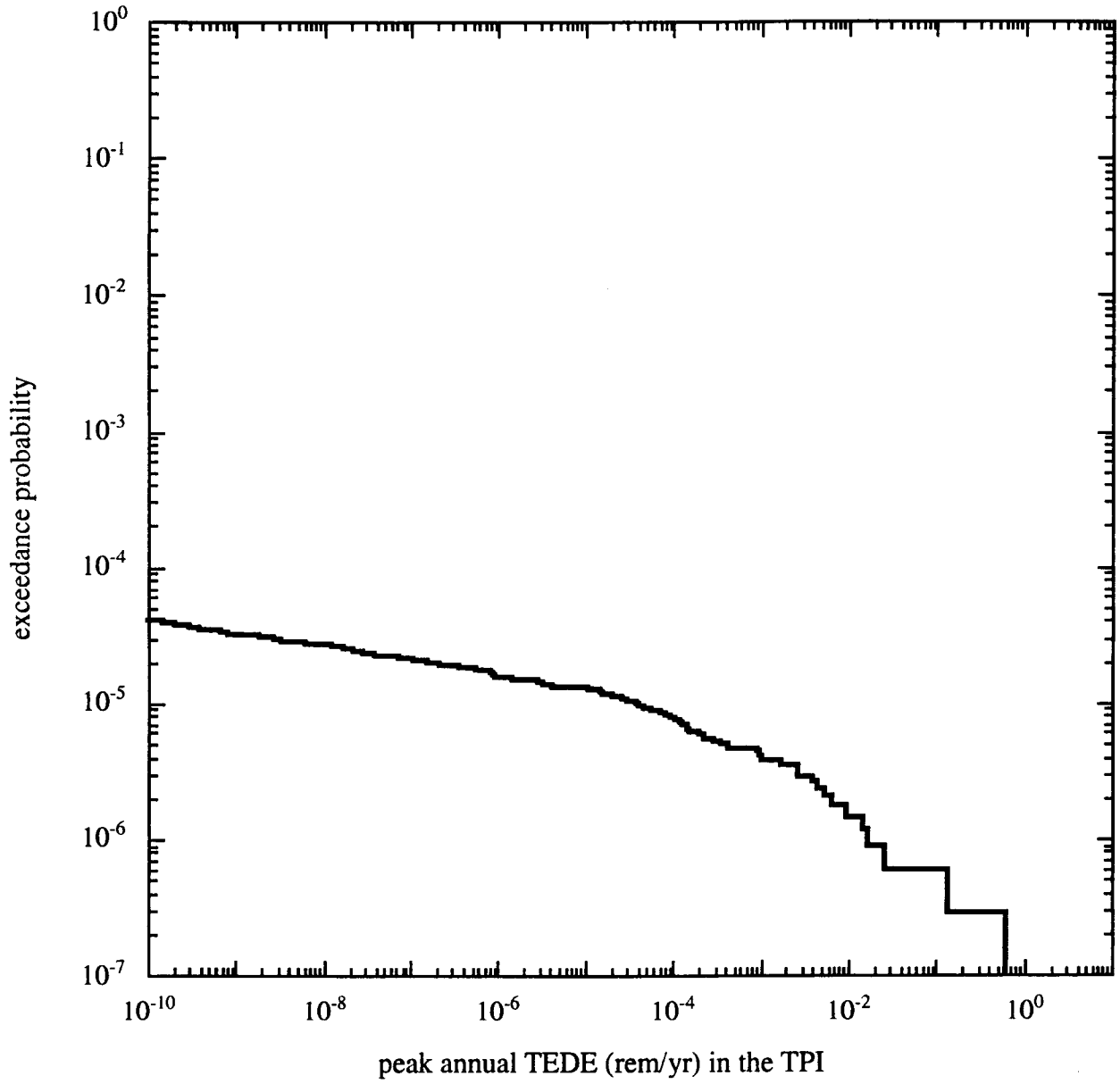


Figure A-5. The CCDF of the peak annual TEDE (rem/yr) at dose point 3 for a TPI of 10,000 yr

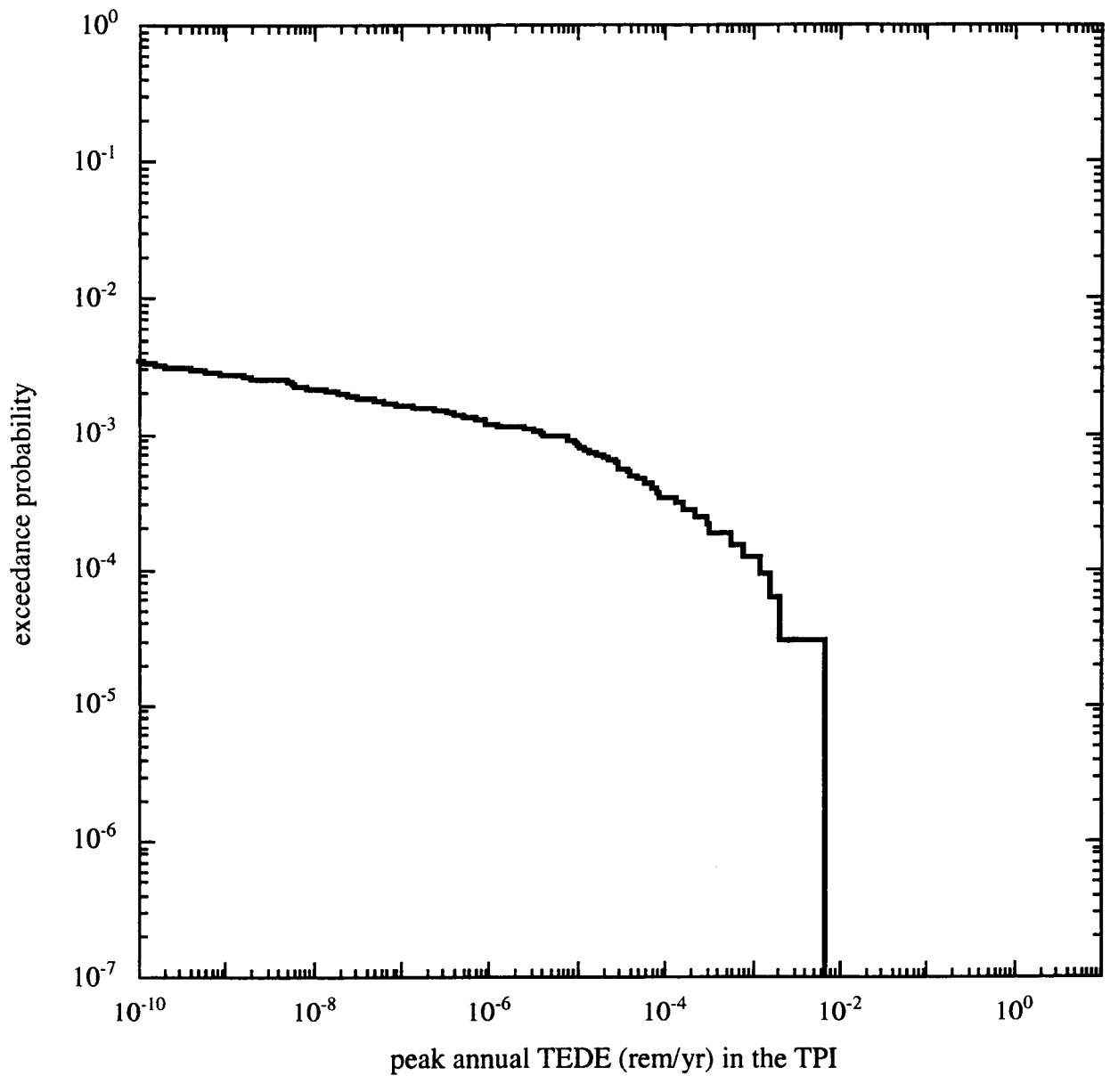


Figure A-6. The CCDF of the peak annual TEDE (rem/yr) at dose point 3 for a TPI of 1,000,000 yr

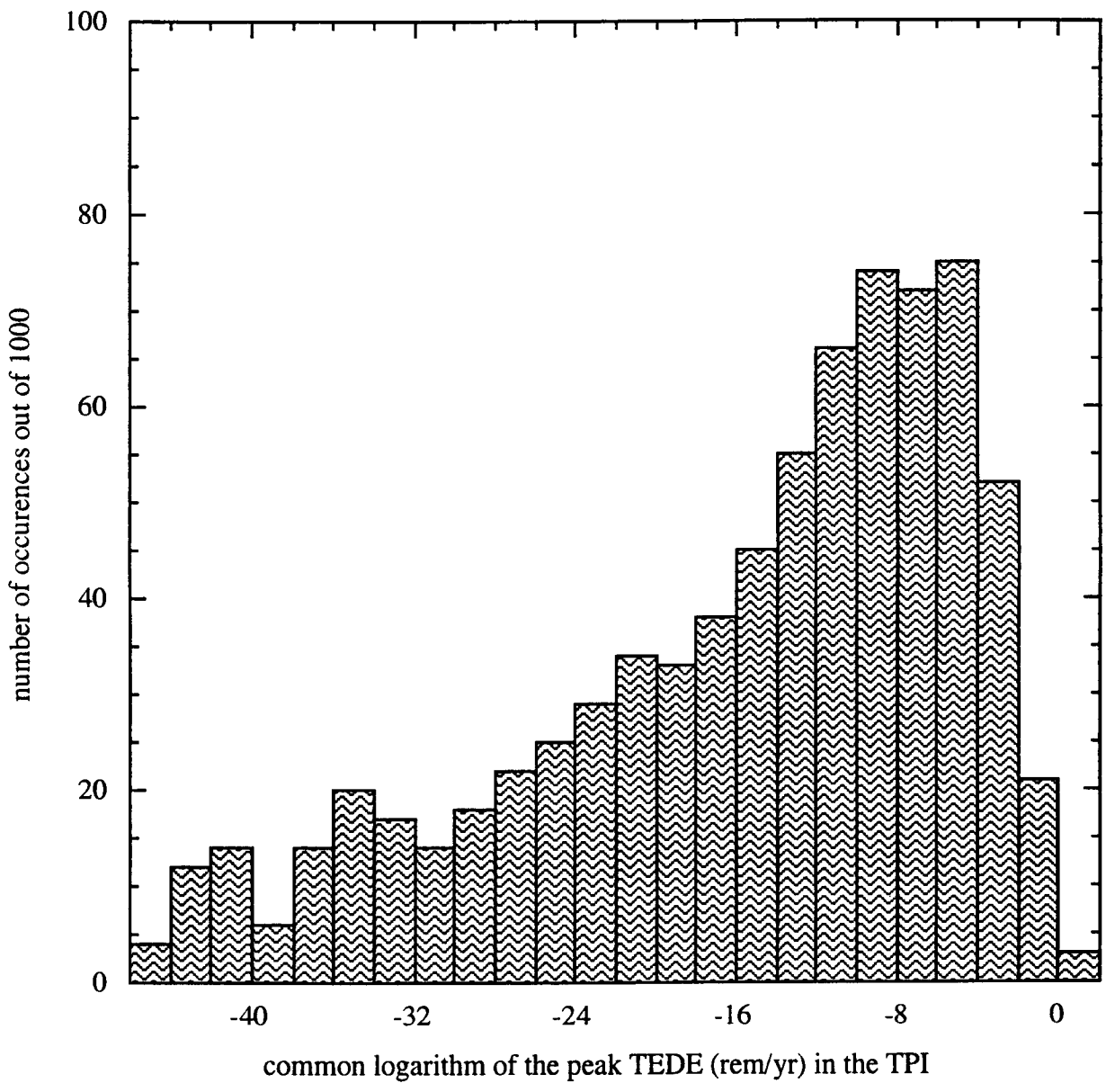


Figure A-7. A stack histogram of the common logarithm of the peak TEDE (rem/yr) at dose point 1 for a TPI of 10,000 yr

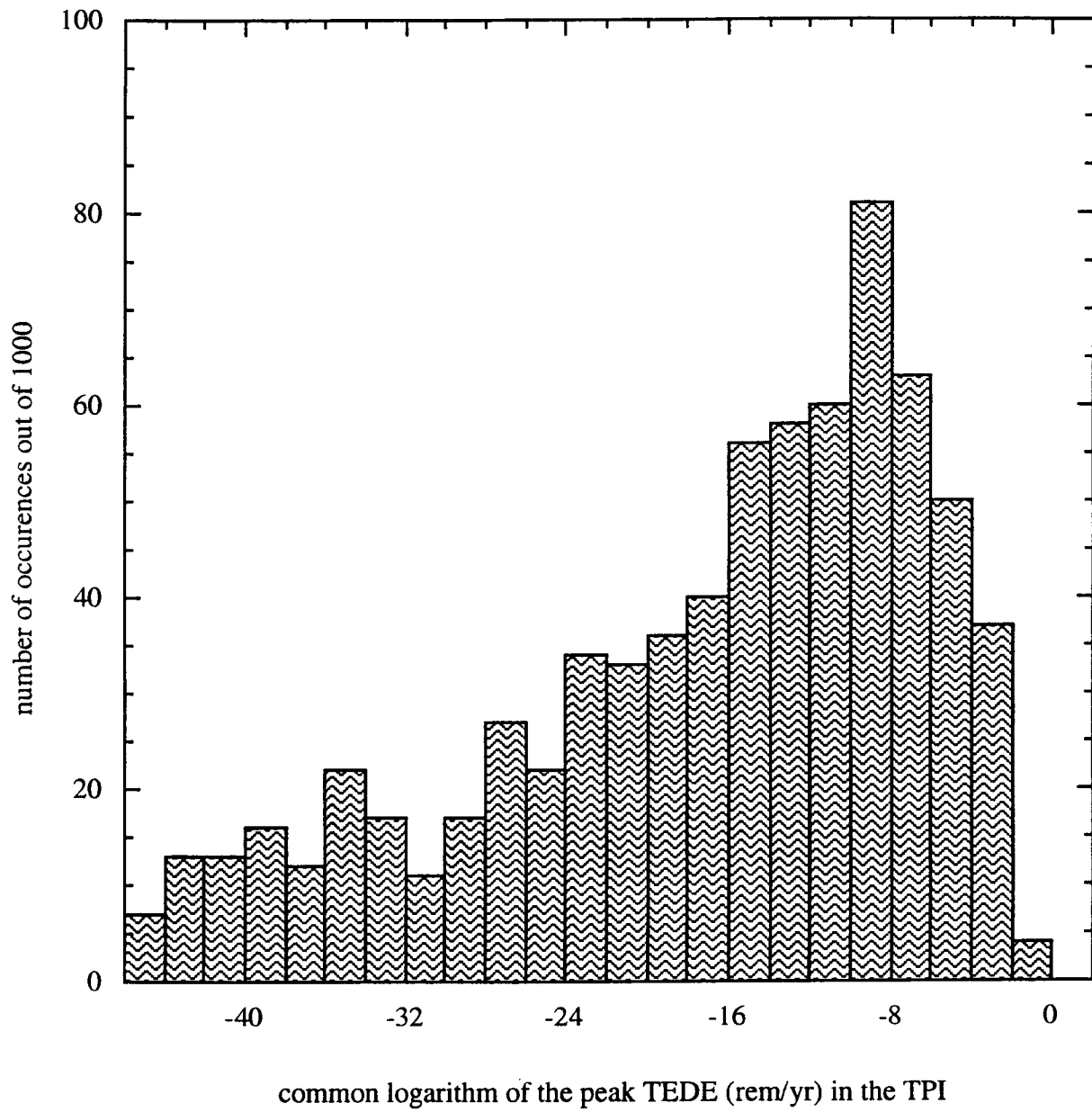


Figure A-8. A stack histogram of the common logarithm of the peak TEDE (rem/yr) at dose point 1 for a TPI of 1,000,000 yr

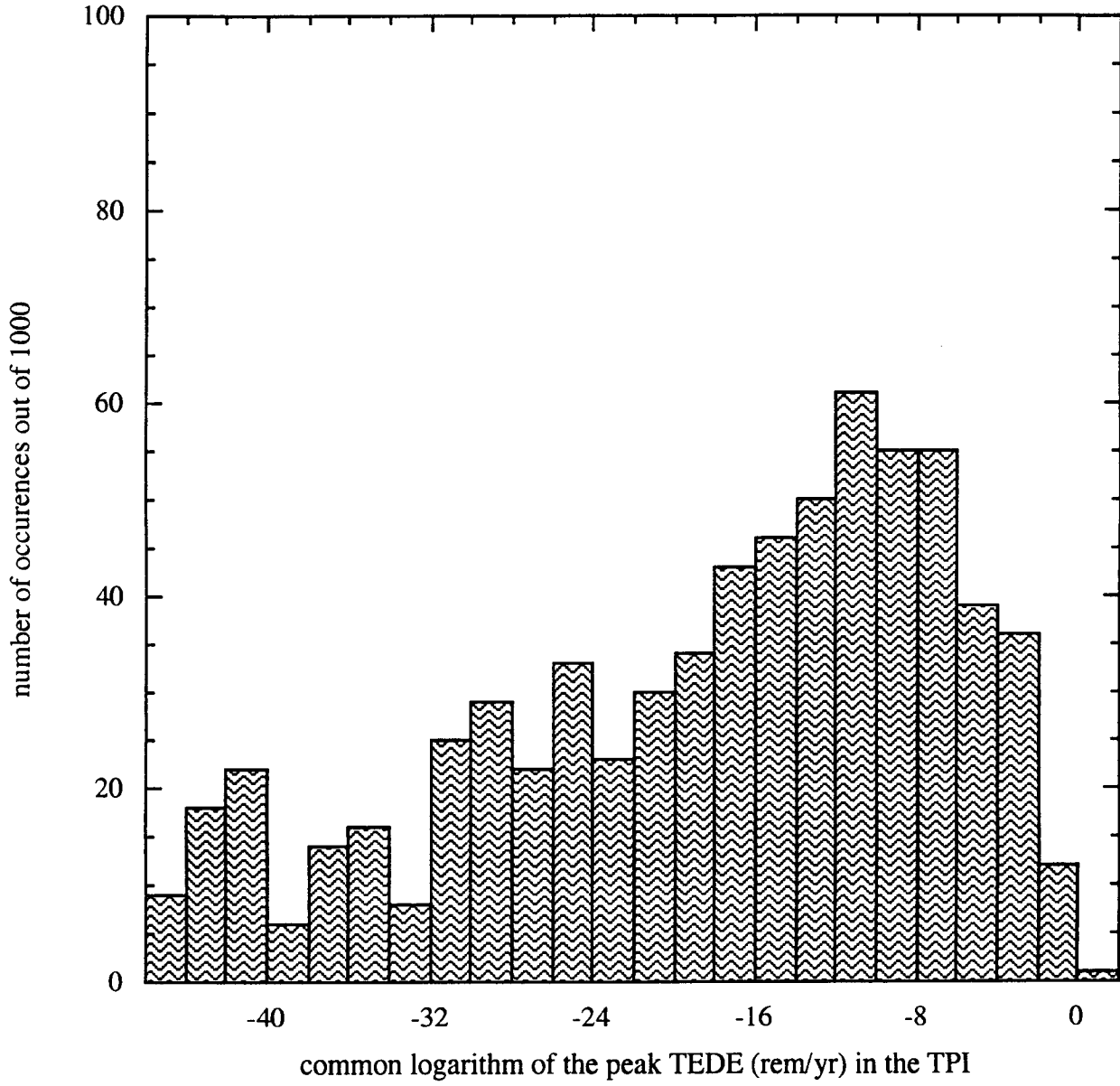


Figure A-9. A stack histogram of the common logarithm of the peak TEDE (rem/yr) at dose point 2 for a TPI of 10,000 yr

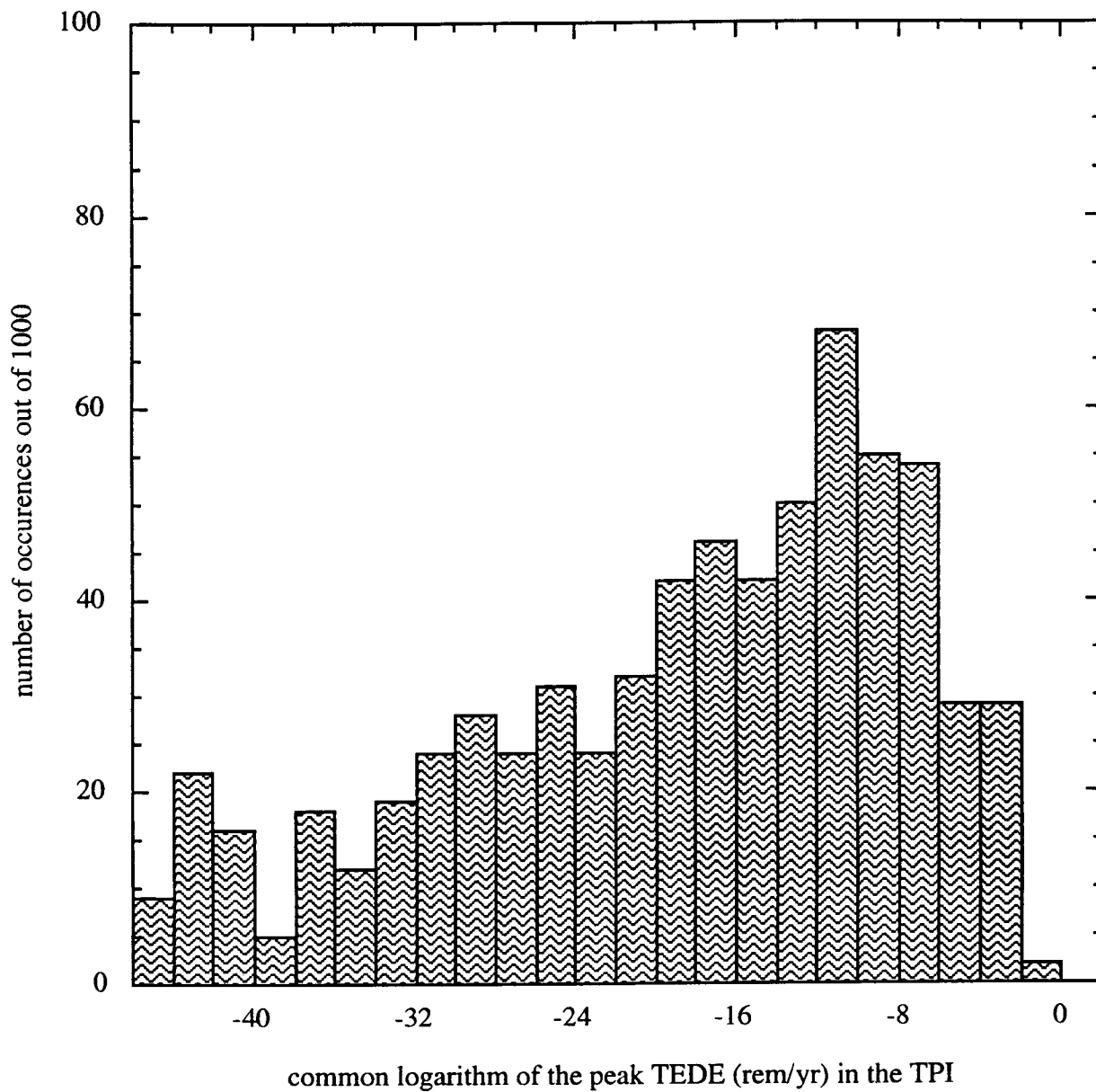


Figure A-10. A stack histogram of the common logarithm of the peak TEDE (rem/yr) at dose point 2 for a TPI of 1,000,000 yr

40/41

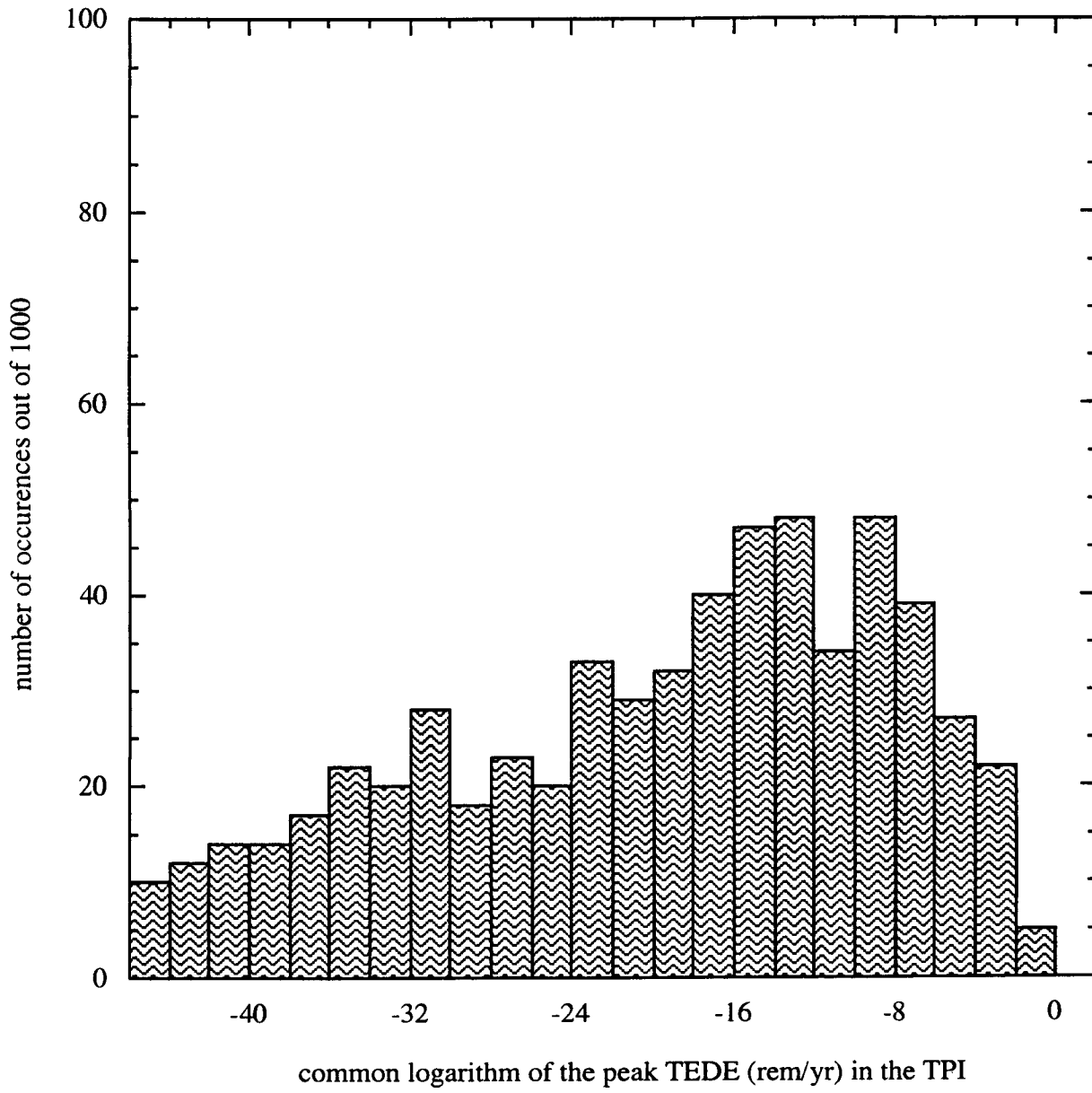


Figure A-11. A stack histogram of the common logarithm of the peak TEDE (rem/yr) at dose point 3 for a TPI of 10,000 yr

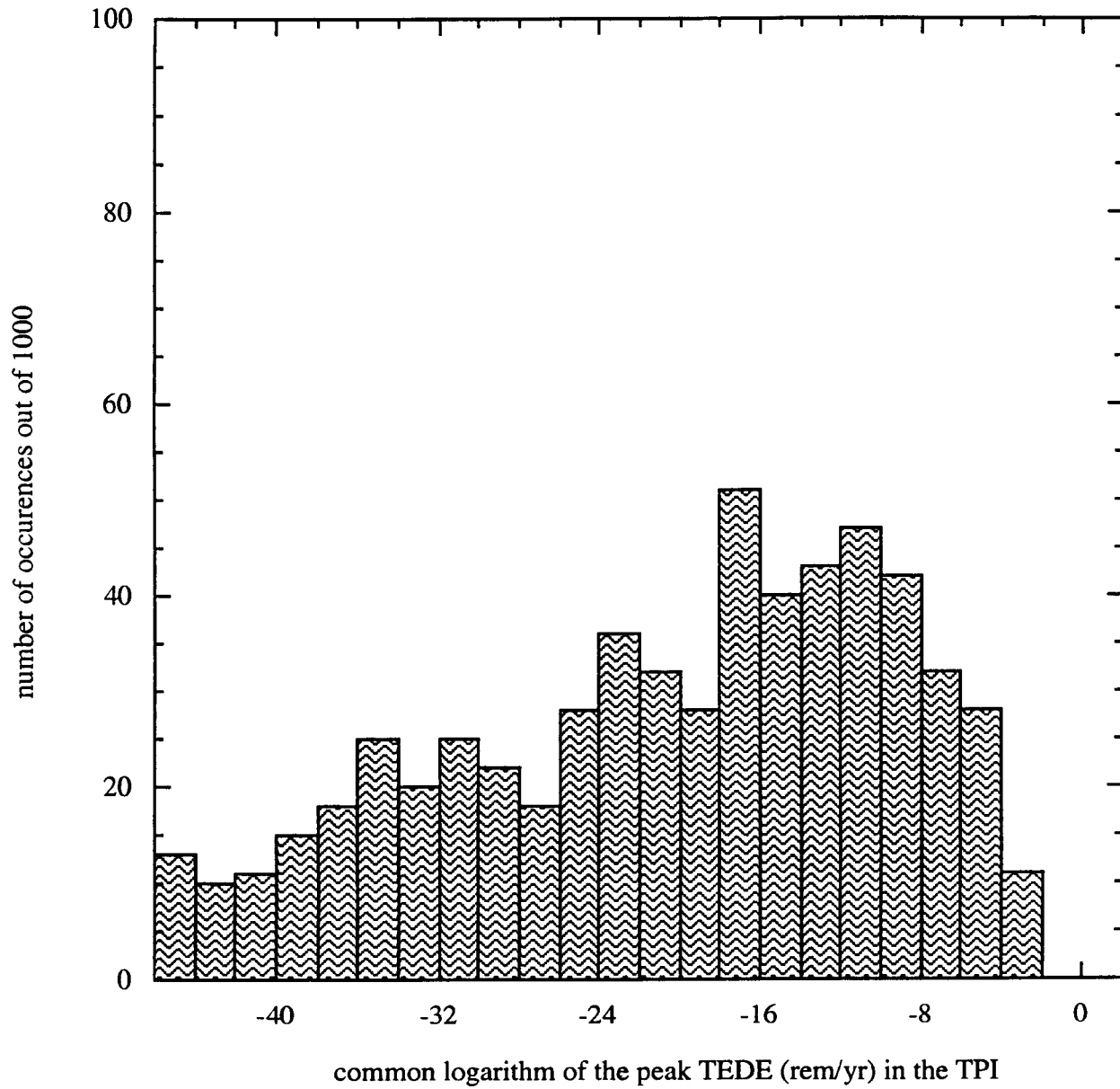


Figure A-12. A stack histogram of the common logarithm of the peak TEDE (rem/yr) at dose point 3 for a TPI of 1,000,000 yr